A glutamate receptor-like gene *AtGLR2.5* with its unusual splice variant has a role in mediating glutamate-elicited changes in *Arabidopsis* root architecture

Yuan-Yong Gong[1, §], Chang-Zheng Wu[1], Yan-Sheng Wu[2], Andrea Alfieri[3], Yu-Cheng Xiang[1], Dong-Xue Shi[1, $], Shuhui Duan[4], Ming-Fa Zhang[4], Xiao-Xu Li[5], Yi-Chen Sun[1, #], Jin Chao[4], Mark Tester[6], Zhonglin Shang[2], Brian G. Forde[7] and Lai-Hua Liu[1, *]

[1]College of Resources and Environmental Sciences, China Agricultural University, Beijing, P.R. China

[2]College of Life Sciences, Hebei Normal University, Shijiazhuang, Hebei, P.R. China

[3]Centro Grandi Strumenti, University of Pavia, Pavia, Italy.

[4]Hunan Tobacco Research Institute (Changsha, Xiangxi), China National Tobacco Corporation Hunan Company, Changsha, China

[5]Tobacco Research Institute of Technology Centre, China Tobacco Hunan Industrial Corporation, Changsha, China

[6]Division of Biological and Environmental Sciences and Engineering, King Abdullah University of Science and Technology, Thuwal 23955, Kingdom of Saudi Arabia

[7]Lancaster Environment Centre, Lancaster University, Lancaster LA1 4YQ, United Kingdom

[§]Present address: Biological and Chemical Engineering College, Panzhihua University, Panzhihua, China

[$]Present address: Dongchangfu Secondary Vocational School, Liaocheng, China

[#]Present address: State Key Laboratory of Vegetation and Environmental Change, Institute of Botany, Chinese Academy of Sciences, Beijing, China

*** Correspondence**

Lai-Hua Liu, College of Resources and Environmental Sciences, China Agricultural University, Yuanmingyuan West Road 2, Haidian District, Beijing 100193, P.R. China

Email: LL1025@cau.edu.cn

Funding information

The National Natural Science Foundation of China (grant no. 30771288 to L-H.L.); the Research Finding of Hunan Tobacco Science Institute (No. 19–22Aa02 and 2022433100240105); the Funding of China Tobacco Genome Project in China Tobacco Hunan

Industrial Corporation (No. KY2022YC0006_110202201012(JY-12)); the European Commission Research Training Network grant no. HPRN-CT-2002-00247 to B.G.F.

Abstract

The occurrence of external L-glutamate at the Arabidopsis root tip triggers major changes in root architecture, but the mechanism of L-Glu sensing is unknown. Members of the family of GLUTAMATE RECEPTOR-LIKE (GLR) proteins are known to act as amino acid-gated Ca^{2+}-permeable channels and to have signaling roles in diverse plant processes. To investigate the possible role of GLRs in the root architectural response to L-Glu, we screened a collection of mutants with T-DNA insertions in each of the 20 *AtGLR* genes. Reduced sensitivity of root growth to L-Glu was found in mutants of one gene, *GLR2.5*. Interestingly, *GLR2.5* was found to apparently produce four transcript variants encoding hypothetical proteins of 169-720 amino acids. One of these transcripts, *GLR2.5c*, encodes a truncated GLR protein lacking both the conserved amino-terminal domain and part of the ligand-binding domain. When a *glr2.5* mutant was transformed with a construct constitutively expressing *GLR2.5c*, both L-Glu sensitivity of root growth and L-Glu-elicited Ca^{2+} currents in root tip protoplasts were restored. These results, along with homology modelling of the truncated ligand-binding domain of GLR2.5c, suggest that GLR2.5c has a regulatory or scaffolding role in heteromeric GLR complex(es) that may involve triggering the root architectural response to L-Glu.

KEYWORDS

root development, glutamate signaling, glutamate receptor-like genes (GLRs), Ca^{2+} channel, homology modelling, reverse genetics.

1 | INTRODUCTION

To explore the soil efficiently, roots have evolved specific mechanisms for sensing and responding to the external presence of mineral nutrients, as part of an adaptive response to local heterogeneity in soil nutrient composition (Drew et al., 1973; Drew, 1975; Robinson, 1994). More recently, it has been reported that root growth in a variety of plant species displays a distinctive response to an organic form of N, the ubiquitous amino acid L-glutamate (L-Glu) (Walch-Liu et al., 2006a; Walch-Liu et al., 2006b; Skobeleva et al., 2011; Kan et al., 2017; Lopez-Bucio et al., 2018). When the primary root tips of these species are exposed to external

L-Glu, root growth is inhibited and root branching stimulated, a response that may enhance the precision of root placement when roots encounter an organic N-rich patch of soil (Walch-Liu et al., 2006b). Detailed studies with *Arabidopsis thaliana* L. have established that the primary effect on the root tip is to inhibit meristematic activity, leading to complete loss of the root meristem after 4 days of L-Glu treatment (Walch-Liu et al., 2006b). Notably, inhibition of root elongation can be seen even at low L-Glu concentrations (≥50 μM in some accessions) and is highly specific to L-Glu, with no other amino acid able to produce the same set of distinctive effects on root tip morphology and root architecture (Walch-Liu et al., 2006b; Forde, 2014). These effects on root development were shown to depend on direct exposure of the primary root tip to L-Glu (Walch-Liu et al., 2006b), implying the existence of an L-Glu sensor in the outer layers of the root apex and a downstream signal transduction pathway leading to inhibition of meristematic activity. A component of this L-Glu-specific signalling pathway has been identified in the form of the MEKK1 MAP kinase kinase kinase, which appeared to act independently of its kinase activity (Forde et al., 2013). More recently another pair of MAP kinases, mitogen-activated protein kinase 6 (MPK6) and the dual specificity serine–threonine–tyrosine phosphatase MKP1, have been identified as additional components of the same pathway (Lopez-Bucio et al., 2018; Ravelo-Ortega et al., 2021). This suggests an analogy with glutamate signalling in animals where signalling mediated by ionotropic glutamate receptors (iGluRs) can be transduced *via* MAP kinase-dependent pathways (Haddad, 2005; Wang et al., 2007; Mao et al., 2009).

Despite progress in identifying downstream components of the L-Glu signalling pathway, the sensor that triggers the morphological response to external L-Glu has remained unidentified. Plants possess a family of glutamate receptor-like *GLR* genes that encode membrane proteins homologous to the mammalian iGluRs (Chiu et al., 2002; Davenport, 2002; Price et al., 2012) and these *GLR* genes have been assigned to three or four plant-specific clades on the basis of phylogenetic analysis (Chiu et al., 2002; Aounini et al., 2012; Liu et al., 2021). Plant GLRs share with iGluRs the same modular structure, consisting of an amino-terminal domain (ATD), a two-lobed S1/S2 ligand-binding domain (LBD), three membrane-spanning segments (M1-M3), a pore region (P) and a C-terminal segment (Chiu et al., 1999; Price et al., 2012; Wudick et al., 2018). Some of the 20 members of the Arabidopsis *GLR* gene family (*GLRs*) have been characterized in detail, both *in planta* and in heterologous systems, providing evidence that they act as amino acid-gated Ca^{2+}-permeable channels (Qi et al., 2006; Stephens et al., 2008; Michard et al., 2011; Vincill et al., 2012; Tapken et al., 2013; Kong et al., 2015;

Alfieri et al., 2020； Wu et al., 2022). However, unlike their largely glutamate-specific iGluR homologues, Arabidopsis GLRs are collectively activated by a diverse set of ligands (Forde & Roberts, 2014; Weiland et al., 2016; Simon et al., 2023) and at least some individual GLRs are apparently gated by multiple amino acids, not necessarily including glutamate.

Recently an important advance was made when it was confirmed experimentally that the LBD of one member of the AtGLR family, AtGLR3.3, is indeed able to bind several different amino acids, including L-Glu (Alfieri et al., 2020), and with the determination by the same authors of the 3D structure of the binding site. The fact that *GLR* gene family is expressed throughout the plant (at least at the mRNA level), with multiple *GLR* genes being expressed in individual cell types (Chiu et al., 2002; Roy et al., 2008) and their gene products localised to different cell compartments (Teardo et al., 2011; Vincill et al., 2013; Teardo et al., 2015), taken together with evidence that plant GLRs can function as heteromers (Price & Okumoto, 2013; Vincill et al., 2013), suggests the potential for a wide diversity in functionally distinct forms of the GLR receptor within the plant.

To date, GLRs have been implicated in a wide range of physiological processes, including aspects of pollen and root development, the response and adaptation to abiotic stresses and the response to pathogens and wounding (Qiu et al., 2020). Reports that specific *GLR* genes in rice (Li et al., 2006) and Arabidopsis (Singh et al., 2016) encode positive regulators of meristematic activity in the root tip are consistent with the suggestion (Walch-Liu et al., 2006b; Walch-Liu & Forde, 2007) that one or more members of the *GLR* gene family could encode the sought-after sensor responsible for triggering the root architectural response to external L-Glu. Here we describe the results of a reverse genetics approach aimed at testing this hypothesis by screening a collection of Arabidopsis mutants carrying T-DNA insertions in members of the *GLR* gene family.

We report that disruption of one gene, *GLR2.5*, leads to a significant reduction in the root's sensitivity to L-Glu and provide evidence that L-Glu sensitivity is conferred by the product of one of four alternative transcripts of *GLR2.5.* This splice variant, *GLR2.5c*, is predicted to encode an unusual, truncated version of the GLR protein lacking most of the ATD and part of the S1 lobe of the LBD. We discuss how our findings fit into and expand our current understanding of the pathway by which Arabidopsis roots sense and respond to environmental glutamate.

2 | MATERIALS AND METHODS

2.1 | Plant material and growth

T-DNA lines with insertions in *GLR* genes were either from the Salk collection (Alonso *et al.*, 2003) held at the European Arabidopsis Stock Centre (NASC), or from the GABI-Kat collection at the University of Bielefeld (Kleinboelting et al., 2012) (see Supporting information Table S1). For testing the plant's sensitivity to L-Glu and hormones, Arabidopsis seedlings (Col 0; CS6000) were germinated and grown aseptically on solid standard nutrient medium (as previously described in Walch-Liu *et al*., 2006b) in vertical Petri dishes (90 mm diameter) at 21°, light intensity 120 µmol/m^2 and 16/8 h light-dark. Seedlings were transferred to fresh medium with and without treatments after 4 d. Note: The growth medium, based on a 50-fold dilution of Gamborg's B5 medium (containing following compositions: 5 mM KCl, 1 mM $CaCl_2 \cdot 6H_2O$, 2 mM $MgSO_4 \cdot 7H_2O$, 1.1 mM NaH_2PO4 1.1，0.18 mM Fe-EDTA, 45 µM $MnSO_4 \cdot 4H_2O$, 7µM $ZnSO_4 \cdot 7H_2O$, 1.03 µM $Na_2MoO_4 \cdot 2H_2O$, 0.105 µM $CoCl_2 \cdot 6H_2O$, 0.1µM $CuSO_4$, 4.5 µM KI, 48.5 µM H_3BO_3. Gamborg et al. 1968), was applied; 1% PhytagelTM was used and 1 mM each of $MgCl_2$ and $CaCl_2$ was added to aid solidification. Amino acids and other nitrogen sources used in solution were filter-sterilized and added to the growth medium after autoclaving.

2.2 | Molecular verification of T-DNA insertion mutants in *GLR* genes

The gene-specific primers used to verify the presence and location of an insert in each T-DNA line are listed in Table S1. Either a 'reverse' primer or a 'forward' primer was used, depending on the orientation of the T-DNA insert with respect to the *GLR* gene, in combination with a left-border T-DNA primer. The left-border primer for SALK lines was 5'-ATGGTTCACGTAGTGGGCCATCG-3', the left-border primer for GABI-Kat lines was 5'-CCCATTTGGACGTGAATGTAGACAC-3'. The Extract-N-Amp™ Tissue PCR Kit (Sigma-Aldrich) was used for quick DNA extraction and PCR amplification according to the manufactory's protocol (https://www.sigmaaldrich.com/SG/en/technicaldocuments/protocol/genomics/pcr/redextract-n-amp), except that the Taq polymerase used was BIOTAQ™ (Bioline). The annealing temperature was 62° and the number of cycles 35-38. The extension time at 72° was 2 min.

2.3 | PCR amplification and cloning of *GLR2.5* transcripts

Total root RNA was subjected to RT-PCR using Easypfu^{TM} DNA Polymerase (Transgen, Beijing) according to the supplier's instructions. Primers were 5'-ATGGCTTCAAGACAAGGATTG-3' and 5'-CTAGAGTTTAGGTTTGACTAT-3', directed at the 5' and 3' ends of the model *GLR2.5* coding sequence from the Aramemnon membrane protein database [https://aramemnon.botanik.uni-koeln.de] (Schwacke *et al.*, 2003). PCR amplification began with 4 min at 94°, followed by 33 cycles of 30 s at 94°, 30 s at 56°, 190 s at 72°, and finally 72° for 10 min. RT-PCR of *Actin2* (At3g18780) was used as an internal control for RNA quality. The *Actin2* primers were 5'-TCCAAGCTGTTCTCTCCTTG-3' and 5'-AGGGCTGGAACAAGACTTCT-3' and the conditions were: 4 min at 95°, followed by 32 cycles of 30 s at 95°, 30 s at 52°, 30 s 72°, followed by 72° for 10 min. The qPCR test (Figure S8) refers to the same protocol in Wang et al. 2012. For cloning of *GLR2.5* transcripts, the RT-PCR products were separated by agarose gel electrophoresis and the four cDNA fragments excised and cloned into pEasy-Blunt (TransGen) for *GLR2.5a* or pGEM-T Easy (Promega) for *GLR2.5b*, *GLR2.5c* and *GLR2.5d*. For the cloning of the RT-PCR transcripts of the individual *AtGLR2.5* splicing variants, at least five clones were sequenced; and the clones derived from the same splicing variant was verified to possess indeed an identical DNA sequence.

2.4 | Generation of transgenic plants and histochemical assay

A 5533 bp fragment carrying the promoter and complete coding sequence of the *GLR2.5* gene was PCR-amplified using the primers 5'-AAGGATCCACTATTTAATGGTGTCATTTCC-3' and 5'-AAGGATCCACTCAAGAAAAATGAGATTGAG-3', cloned into the pGEM-T Easy vector and verified by sequencing. The genomic fragment (*GLR2.5g*) was transferred to the pCAMBIA2300 Agrobacterium binary vector (Abcam, Shanghai, China) and used to transform the *glr2.5-1* mutant to generate complemented *glr2.5-1*/*GLR2.5g* lines. Kanamycin-resistance and RT-PCR were applied to select homozygous lines (*glr2.5-1*/*GLR2.5g*) into the T3 generation for experimental use. To generate *glr2.5* mutant lines expressing the *GLR2.5c* cDNA (*glr2.5-1*/*35S::GLR2.5c* lines), the *GLR2.5c* sequence was introduced downstream of the enhanced CaMV 35S promoter (Kay *et al.*, 1987) in the pGreen0229 binary vector and used to transform the *glr2.5-1* mutant, and homozygous T3 lines were selected. To generate *GLR2.5* reporter lines, its promoter region (*GLR2.5pro*) was cloned by PCR using Phusion® High-Fidelity DNA polymerase (New England Biolabs) and the primers 5'-ACTATTTAATGGTGTCATTTCCTTC-3' and 5'-TATGAGTATTATAAAATTCCGACAGA-3'. Reaction conditions were according to the

supplier's instructions and the temperature regime was: 98° 30 s followed by 35 cycles of 98° 10 s, 60° 30 s, 72° 150 s and finally 72° for 10 min. The 1846 bp GLR2.5pro fragment was cloned into pGEM-T Easy and verified by DNA sequencing before transferring to the pGreen0229-*35S::GUS* binary vector (Hellens *et al.*, 2000), replacing the 35S promoter with GLR2.5pro. Several T_2 transgenic lines were obtained based on kanamycin-resistance segregation analysis. For GUS staining-based histochemical experiments, a detailed method exactly refers to Zheng et al. (2019). The GUS staining solution contains following chemical compositions: 25 mM sodium phosphate buffer at pH 7.0, 10 mM EDTA, 0.5 mM ferricyanide, 0.5 mM ferrocyanide, 0.1% Triton X-100, and 2 mM X-Gal (5-bromo-4-choro-3-indolyl-β-d-glucuronide cyclohexylamine salt).

2.5 | Isolation of Arabidopsis root tip protoplasts

Surface-sterilized seeds of each line (Col-0, the *glr2.5-1* mutant and the T3 generation of the complemented lines, *glr2.5-1*/*GLR2.5g* and *glr2.5-1*/*35S::GLR2.5c*) were germinated and grown vertically for 15 d on nutrient agar plates. Protoplasts were prepared from primary root tips of 15 d-old seedlings. About 150 root tips ~1 mm in length were excised, chopped further into as shorter pieces as possible and treated with 1 mL of enzyme solution consisting of 0.5% cellulase R-10 (Yakult, Japan), 0.5% cellulysin (Sigma-Aldrich, USA), 0.2% pectolyase Y-23 (Yakult, Japan), 20 mM $CaCl_2$, 5 mM MES [2-(N-morpholino)-ethanesulphonic acid], pH 5.8. Samples were gently shaken in the enzyme solution at 28° and 70 rpm for 90 min. The enzyme solution was filtered using a nylon mesh with 30 μm pores, and then centrifuged for 5 min at 200 g. Protoplasts (~0.2 mL) were collected at the bottom of the centrifuge tube and resuspended with 1.5 mL fresh solution consisting of 20 mM $CaCl_2$, 5 mM MES, pH 5.8. All solutions were adjusted to 290-300 mOsm·Kg^{-1} with D-sorbitol and the isolated protoplasts were stored on ice for up to several hours before their use in electrophysiological experiments.

2.6 | Electrophysiology

The bathing solution for patch-clamp experiments consisted of 20 mM $CaCl_2$, 5 mM MES, pH 5.8 (adjusted with Tris). The pipette solution consisted of 0.5 mM $CaCl_2$, 8.5 mM $Ca(OH)_2$, 2 mM Mg·ATP_2, 0.5 mM Tris·ATP, 10 mM 1,2-Bis (*2*-aminophenoxy*)* ethane-N,N,N′,N′′-tetraacetic acid *(*BAPTA), 15 mM Hepes, pH 5.8 (adjusted with Tris). All patch-clamp solutions were adjusted to 290-300 mOsm·Kg^{-1} with D-sorbitol. Glass pipettes (World Precision Instruments) were pulled using a vertical puller (Model PC-10, NARISHIGE, Japan).

The whole-cell voltage clamping configuration was used and an AXON 700B amplifier (AXON Instruments, USA), controlled by Clampex 10.3 software (AXON Instruments, USA) recorded the current signal, the data being sampled at 1 kHz and filtered at 200 Hz (Véry & Davies, 2000). The voltage-clamp protocols consisted of a series of 1.5 s depolarizing and/or hyperpolarizing steps from a holding potential of 0 to -200 mV. Current-voltage relationships (*I-V* curves) were constructed from total whole-cell currents that were measured following the 1.5 s voltage clamp. For slow-ramp voltage clamping, the voltage was changed from -200 to 0 mV in 20 s. The data were analysed and plotted using Microcal Origin 6.0 software.

2.7 | 3D structural representations and homology modelling

The models of GLR2.5 and GLR2.5c were generated using the online server SWISS-MODEL [swissmodel.expasy.org] (Waterhouse et al., 2018) providing as input the structure of GLR3.3 LBD + L-Glu at 2.0-Å resolution (Protein Data Bank ID code 6R85, Alfieri et al., 2020). Final model quality was assessed by the MolProbity score and QMEAN Z-score included in SWISS-MODEL calculations (Benkert et al., 2011).

3 | RESULTS

3.1 | Identification of a *GLR* mutant with reduced sensitivity to L-Glu

We have mined the SALK (Alonso et al., 2003) and GABI-Kat (Rosso et al., 2003) populations of Arabidopsis T-DNA lines to isolate a set of 27 homozygous mutants with insertions in *GLR* genes, at least one for each of the 20 members of the *GLR* gene family (Table S1). When each of these 27 mutants was tested by growth on medium with and without L-Glu under our experimental conditions, insertions in one gene, *GLR2.5*, were found to affect the root's sensitivity to this amino acid (Figure 1. see later in discussion 4.1).

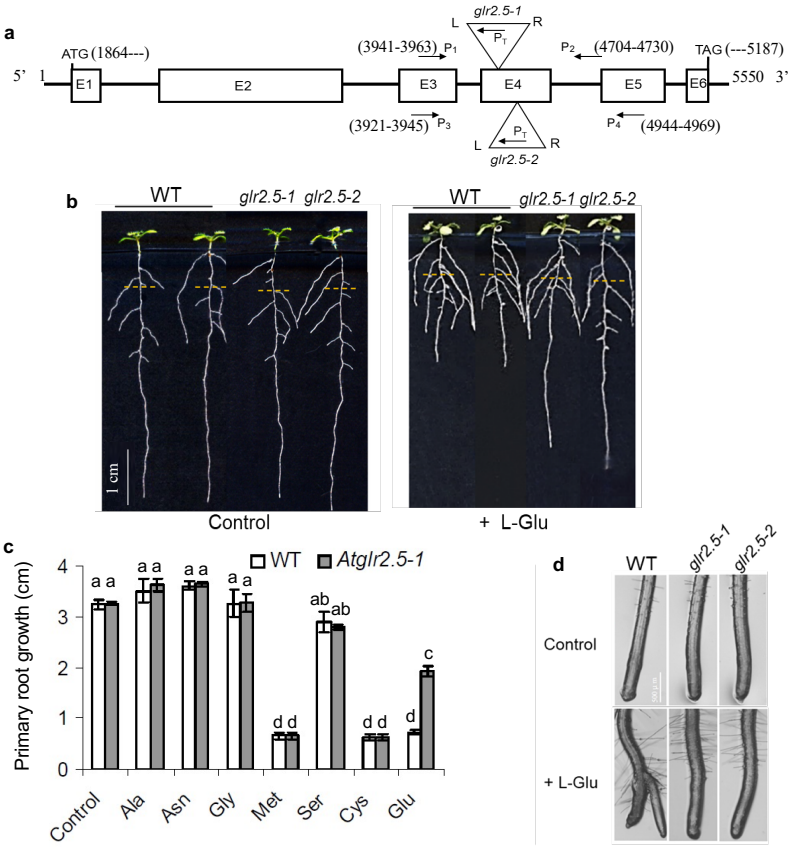

FIGURE 1 Disruption of the *GLR2.5* gene in two independent Arabidopsis T-DNA lines leads to reduced glutamate sensitivity in primary root development. (**a**) Schematic representation of two independent T-DNA insertion events in *GLR2.5* (At5g11210). The arrangement of exons (E1-E6) is based on the model in the Aramemnon database [https://aramemnon.botanik.uni-koeln.de]. The T-DNA insertions in the *glr2.5-1* and *glr2.5-2* lines (NASC accession nos N578407 and N618122) are located respectively 2431 bp and 2585 bp downstream of the predicted start of translation. Numbered arrows (P_1, P_2 for *glr2.5-1* and P_3, P_4 for *glr2.5-2*) indicate annealing sites and orientations of PCR primers used to detect T-DNA insertions and in homozygosity tests (for primer sequences see Table S1); P_T indicates the T-DNA primer annealing site. The numbers indicate the nucleotide positions in the genomic sequence of *AtGLR2.5* predicted by the Aramemnon database [https://aramemnon.botanik.uni-koeln.de]. The expected DNA fragment size is 790 bp or 1049 bp between primer P_1 and P_2, or P_3 and P_4. L and R, left and right T-DNA borders. (**b**) Representative image showing seedlings of WT (Col-0) and the *glr2.5-1* and *glr2.5-2* mutants that were germinated and grown for 4 d on vertical agar plates containing "standard medium" (Walch-Liu et al., 2006b) and then transferred to plates ±1 mM L-Glu for a further 6 d (see Materials and Methods). Horizontal dotted lines show the positions of the primary root tips at the time of transfer. (**c**) Effect of other amino acids on root growth in the wild-type and the two *glr2.5* mutants. The experiment

was conducted as for the L-Glu treatment in b, except that the respective amino acids were applied at a concentration of 0.5 mM. Data are means ± SE (n =18 plants); different letters above bars indicate statistically significant differences ($P < 0.05$, by one-way ANOVA). (**d**) Close-ups of representative primary root tips of each line grown in the absent (Control) or presence of 1 mM L-Glu. Root materials were derived from the experiment for b.

Figure 1a illustrates diagrammatically the location of the T-DNA inserts in two independent *glr2.5* mutants, both of which were within exon 4 and neither of which produced detectable *GLR2.5* transcripts (as detailed below). Figure 1b and Figure S1 demonstrate the reduced sensitivity of roots of the *glr2.5-1* and *glr2.5-2* mutants to growth on 1 mM L-Glu compared to the wild-type. Col-0 seedlings showed the typical response to L-Glu (Walch-Liu et al., 2006b), which includes a marked inhibition of primary root growth and a stimulation of root branching, while both traits were strongly diminished in the mutants (e.g. primary root growth inhibition rate by approximately 35% versus 78% for wild-type. Figure 1b, c). Sensitivity to other amino acids that inhibit root growth at sub-millimolar concentrations (methionine and cysteine) was unaffected by the *glr2.5* mutation (Figure 1c), demonstrating that GLR2.5 regulate the growth of the root specifically in response to L-Glu and not to other amino acids. It was also established that the mutant phenotype was independent of the background N source used for the L-Glu treatments (Figure S2).

Unlike some *GLR* mutants that have previously been characterized in Arabidopsis (Medvedev, 2018) and rice (Li et al., 2006), whose root growth and root tip morphology were affected by disruption to the primary root meristem, the *glr2.5* mutants showed no alteration in root growth or branching when cultured under standard growth conditions (Figure 1b). Close-up observation of root tips of the *glr2.5* mutants also found no significant differences from the wild-type when grown in the absence of L-Glu (Figure 1d).

Previous evidence has implicated auxin signaling and/or transport in the root response to L-Glu (Walch-Liu et al., 2006b; Lopez-Bucio et al., 2018; Ravelo-Ortega et al., 2021), and roles for abscisic acid (Kang et al., 2004; Duan et al., 2015) and gibberellic acid (Ju et al., 2020) have been indicated in other GLR-mediated signaling pathways. When the *glr2.5* mutants were tested for their response to range of concentrations of indole acetic acid, cytokinin (benzyladenine), abscisic acid and gibberellic acid, no effects of the mutation on the root's sensitivity were found (Figure S3).

3.2 | Transformation with a GLR*2.5* genomic clone complements the *glr2.5* mutation

To confirm that the mutant phenotype was specifically due to the disruption of the *GLR2.5* gene, a rescue experiment was carried out in which the *glr2.5-1* mutant was transformed with a genomic fragment carrying the *GLR2.5* gene and its flanking sequences. Based on the gene model of *GLR2.5* in the Aramemnon membrane protein database [https://aramemnon.botanik.uni-koeln.de], a 5533 bp genomic sequence carrying the *GLR2.5* gene was PCR-amplified and cloned. This fragment (*GLR2.5g*) included the promoter region beginning 1846 bp upstream of the predicted translation initiation codon and extending 363 bp downstream of the predicted translation stop codon. The genomic sequence was introduced into the *glr2.5-1* mutant by *Agrobacterium* transformation and two independent complemented lines (*glr2.5/GLR2.5g-1* and *glr2.5/GLR2.5g-2)* were identified.

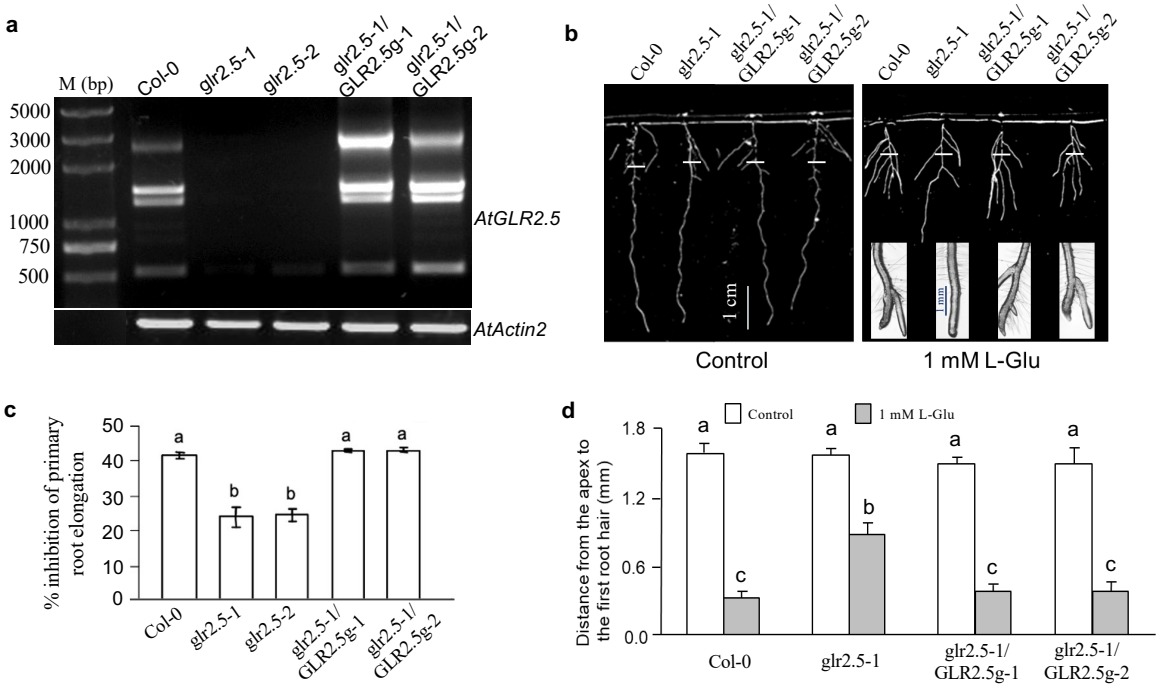

FIGURE 2 Complementation of a *glr2.5* mutant by transformation with the *GLR2.5* gene. A construct carrying the *GLR2.5* gene as a 5533 bp genomic fragment *(GLR2.5g*) was used to transform the *glr2.5-1* mutant and two independent transgenic lines (*glr2.5*/*GLR2.5g-1* and *glr2.5*/*GLR2.5g-2*) were analyzed. (**a**) Detection of *GLR2.5* gene transcription. RT-PCR was performed on total RNA extracted from seedlings of the *glr2.5-1* and *glr2.5-2* mutants and from the two complemented lines as well as wide-type Col-0 (see Materials and Mehtods). PCR products were separated by gel electrophoresis and stained with ethidium bromide. Upper panel: products obtained using PCR primers designed to amplify the complete *GLR2.5* coding sequence; lower panel: RNA quality control showing products obtained with *Actin2* primers.

M, DNA marker. (**b**) Representative images of seedlings of Col-0, the *glr2.5-1* mutant and the complemented lines when 4 d-old seedlings were grown on vertical agar plates and transferred to plates ± 1 mM L-Glu for a further 6 d (see Materials and Methods). Horizontal lines show the positions of the primary root tips at the time of transfer. (**c**) Quantification of primary root growth. Plant data derived from the same experiments as for b. Primary root elongation over the following 5 d was measured, and percentage inhibition by L-Glu was calculated for each genotype by comparison with the control (no L-Glu) plates (± SE; n= 18 plants). Different letters above bars indicate statistically significant differences ($P < 0.05$, by one-way ANOVA). (d) Data showing the effect of L-Glu on meristematic activity in each line as measured by the mean distance from the root apex to the first root hair (± SE; n= 6-8 seedlings). Different letters above bars indicate statistically significant differences ($P < 0.05$, by one-way ANOVA).

These were found by RT-PCR to express a multiple set of *GLR2.5* transcripts that matched those seen in the wild-type and that were almost missing in the *glr2.5* knock-out mutants (Figure 2a. In the case of *glr2.5-2*, a very faint DNA fragment with around 500 bp could still be observed). The images of seedlings grown on medium with and without L-Glu (Figure 2b) show how L-Glu sensitivity of primary root elongation in both complemented lines was restored to wild-type levels. A sensitive measure of the L-Glu phenotype is the appearance of root hairs and the emergence of lateral roots close to the primary root apex, which are traits associated with the strong reduction in meristematic activity at the primary root tip after exposure to L-Glu (Walch-Liu et al., 2006b). The inset images in Figure 2b, and the quantitative data for proximity of root hairs to the root apex in Figure 2c, illustrate how these traits are restored in the complemented lines, confirming that disruption of the *GLR2.5* gene is indeed responsible for the mutant phenotype.

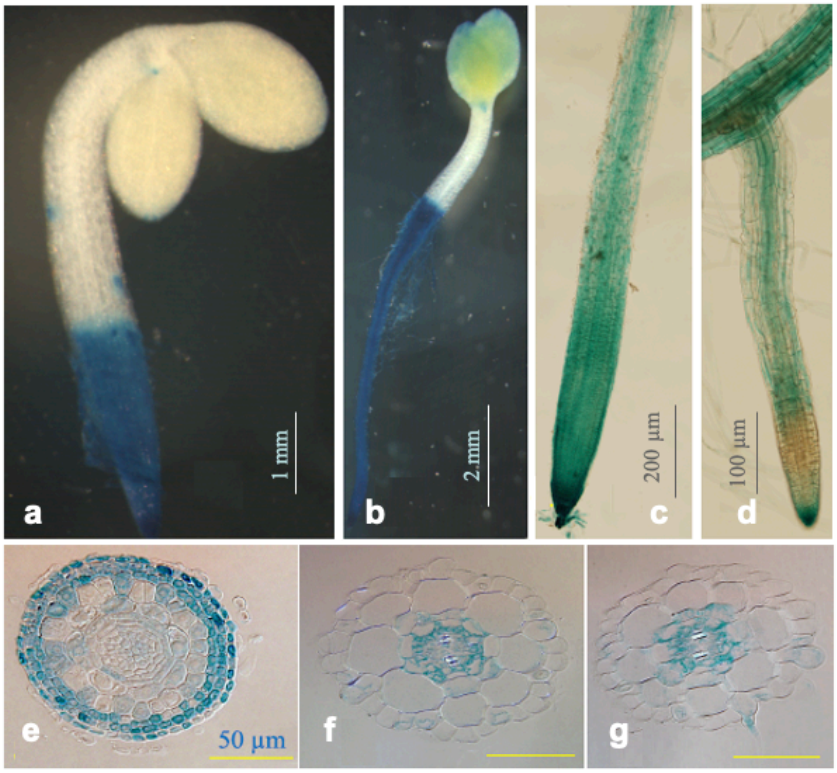

FIGURE 3 Histochemical analysis of transgenic seedlings carrying the *GLR2.5pro::GUS* construct. Seedlings were germinated and grown on vertical agar plates containing standard nutrient medium and stained in 2 mM 5-bromo-4-chloro-3-indolyl β-d-glucuronide salt (X-Gal) at 37° for 2 h incubation (Zhang et al., 2019). (**a**) Seedling 2 d after germination. (**b**) Seedling 3 d after germination. (**c**) Primary root of 8 d-old seedling. (**d**) Lateral root of 8 d-old seedling. (**e-g**) Transverse sections of the primary root apex of 8 d-old seedlings in the meristematic region (**e**) elongation zone (**f**) and root hair zone (**g**).

3.3 | *GLR2.5* is expressed in the outer layers of the primary root apex zone

To investigate the pattern of expression of the *GLR2.5* gene in roots, we placed an 1846 bp fragment containing its promoter region upstream of the β-glucuronidase (GUS) reporter gene and used this to transform Arabidopsis (Col-0 background). Histochemical analysis of the *GLR2.5pro::GUS* lines showed that expression in seedlings was strongest in the root and particularly in the outer cell layers of the root tip or apex region (Figure 3).

3.4 | Multiple alternative transcripts specified by *GLR2.5*

Previous evidence, from electrophoretic analysis of the products of RT-PCR, has indicated that the *GLR2.5* gene is expressed as multiple transcripts (Chiu et al., 2002), an observation

confirmed above when RT-PCR was used to verify the *glr2.5* KO lines (Figure 2a). To characterize these transcripts in more detail, the four products of the RT-PCR reaction (Figure 4a) were cloned and sequenced, revealing that the amplified cDNAs (*GLR2.5a*, *GLR2.5b*, *GLR2.5c* and *GLR2.5d*) were 2605 bp, 1451 bp, 1250 bp and 527 bp in length, respectively (Figure 4b).

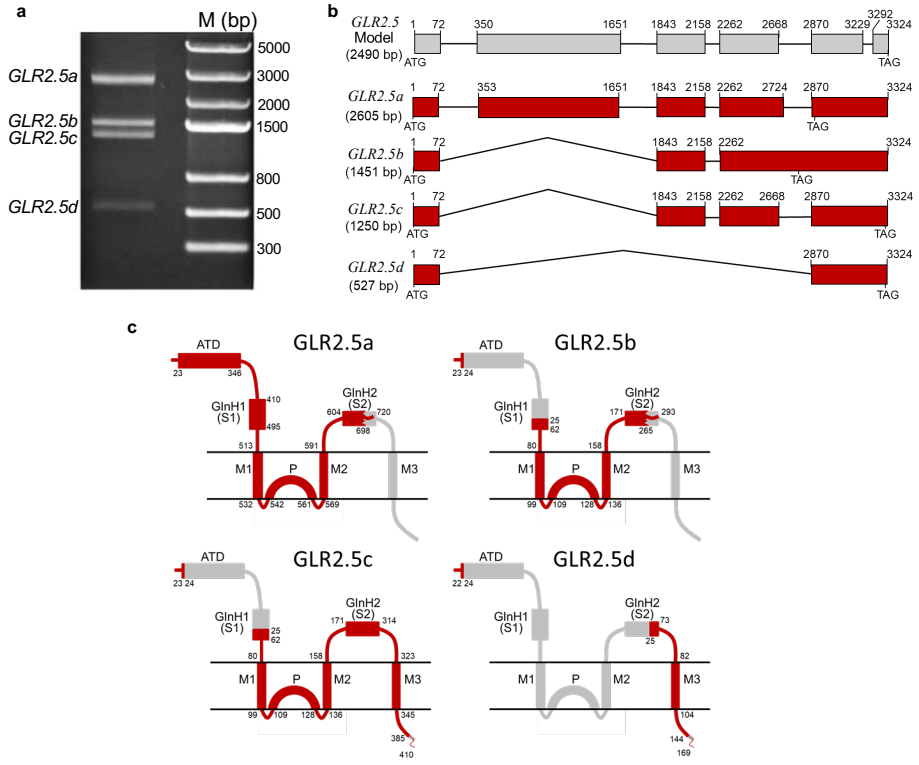

FIGURE 4 Cloning and characterization of four alternative *GLR2.5* transcripts. (**a**) RT-PCR was performed on total RNA from Arabidopsis seedlings to amplify the coding region of the *GLR2.5* gene and the products electrophoresed on agarose gels alongside a set of DNA markers (M) and stained with ethidium bromide. The four PCR products (*GLR2.5a*, *GLR2.5b*, *GLR2.5c* and *GLR2.5d*) were cloned and sequenced (Genbank accession nos JF838182, JF838183, JF838184 and JF838185, respectively). (**b**) Diagrammatic representation of the predicted arrangement of exons in *GLR2.5* based on the Aramemnon gene model (grey) [https://aramemnon.botanik.uni-koeln.de] and as seen in the four alternative transcripts (red). Numbering is from the start of the ATG codon in the *GLR2.5* genomic sequence and positions of the TAG stop codons in each transcript are indicated. Where exon skipping has occurred the intron is shown as an angled line. (**c**) Schematic diagram indicating the presence and absence of the conserved domains common to plant GLRs and animal iGluRs (see text and Figure S5) in the hypothetical translation products of each of the four alternative transcripts. Sequences present in each protein sequence are indicated in red, and sequences absent compared to the

model are in grey. Where a frameshift occurs, this is indicated by a jagged line and the following 'nonsense' sequence by a wavy red line (see GlnH2 (S2) domain of 2.5a and 2.5b). Note: Numbering is from the N-terminus of the model GLR2.5 protein sequence (Aramemnon) and the conserved domains and their spacing are not drawn to scale. The ligand-binding subdomain GlnH1 (S1) and GlnH2 (S2) are considered to have evolved early from periplasmic binding proteins of bacteria due to their significant primary sequence similarity (Nakanishi et al., 1990).

Comparison of the four sequences with the model 2490 bp cDNA sequence and the *GLR2.5* genomic sequence (see Figure S4), confirmed that all four transcripts are derived from the *GLR2.5* gene and that their differing lengths are attributable to the use of alternative splice sites (all of which conform to the GT-AG convention for donor and acceptor sites). As illustrated schematically in Figure 4b, based on a gene model of *GLR2.5* predicted in Aramemnon, the four alternative transcripts are generated from a combination of three different types of event: exon skipping (exon 2 skipped in *GLR2.5b* and *GLR2.5c*, exons 2, 3 and 4 skipped in *GLR2.5d*), intron retention (intron 4 is unspliced in GLR2.5b) and use of alternative splice donor sites (at the 5' end of intron 4, comparing *GLR2.5a* and *GLR2.5c*). Intron 5 predicted in the Aramemnon model is not spliced in any of the alternative transcripts. Although *GLR2.5a* is the most similar in length to the model cDNA (2605 bp vs 2490 bp), it diverges from the model in two additional respects, specifically the acceptor site in intron 1 is three nucleotides downstream of that predicted (maintaining the reading frame), and the donor site in intron 4 is 56 bp downstream of that predicted, leading to a change in the reading frame and an early TAG stop codon.

The open reading frames in *GLR2.5a*, *GLR2.5b*, *GLR2.5c* and *GLR2.5d* are predicted to encode polypeptides of 720, 293, 410 and 169 amino acids, respectively, each of which is significantly shorter than the 829 amino acids of the Aramemnon-predicted sequence. According to the analysis in the Aramemnon database [https://aramemnon.botanik.uni-koeln.de], the model GLR2.5 polypeptide is a conventional GLR protein, possessing all the conserved sequences and functional domains that are common to other plant GLRs and animal iGluRs (Turano et al., 2001; Wudick et al., 2018). (Note that wherever we refer to the *GLR2.5* transcript or its encoded GLR2.5 protein here, the reference is specifically to the model amino acid sequence as defined in the Aramemnon database and shown in Figure S5). However, each of the products of the cloned GLR2.5 transcripts, when aligned with the sequence of the hypothetical *GLR2.5* transcript are found to lack one or more of these conserved sequences

(Figure S5). Figure 4C illustrates schematically how the domain structures of the four polypeptides differ from the model GLR2.5 sequence. All predicted polypeptides contain at least one of the conserved segments that characterize members of the GLR family (Acher & Bertrand, 2005; Wudick et al., 2018), and where a splicing event creates a frameshift relative to the model sequence (as it does in all four transcripts), only relatively short 'nonsense' sequences are created at the C-terminus (Figure 4C and Figure S5). The GLR2.5a isoform is truncated in the middle of the S2 segment, due to a frameshift, so lacks the M3 segment and the subsequent C-terminal region, instead having a novel C-terminal peptide of 20 amino acids. The GLR2.5b isoform is truncated at the C-terminus in the same way, but additionally lacks the ATD and the first part of the S1 segment. The GLR2.5c isoform is the only one to have all three transmembrane regions, the P region and a conventional C-terminal domain, but like GLR2.5b it lacks the ATD and the first part of the S1 segment. The small GLR2.5d isoform consists only of the C-terminal end of S1 along with M3 and a C-terminal domain.

3.5 | The *GLR2.5c* cDNA can complement the *glr2.5* mutant

GLR2.5c represents the only *GLR2.5* transcript able to encode a protein having both an intact P region and all three transmembrane segments, and so was judged to be the only one likely to be both correctly incorporated into the membrane and able to form a functional channel. This cDNA was therefore selected to investigate whether on its own, in the absence of the other major three transcripts, it was able to rescue the *glr2.5* mutant. The *GLR2.5c* sequence was placed under the control of the enhanced CaMV 35S promoter (Kay et al., 1987) and used to transform the *glr2.5-1* mutant. When two independent transformants were grown alongside the wild-type and the two *glr2.5* mutants on plates containing 1 mM L-Glu, the mutant lines expressing the *35S::GLR2.5c* construct were found to have regained wild-type levels of sensitivity to L-Glu (Figure 5a,b). These results suggest that it is loss of the *GLR2.5c* transcript and its encoded polypeptide in *glr2.5* mutants that is solely responsible for the reduction in sensitivity of their primary root tips to external L-Glu. No complementation was obtained when the same analysis was performed with *GLR2.5a*, *GLR2.5b* and *GLR2.5d* (Figure S6).

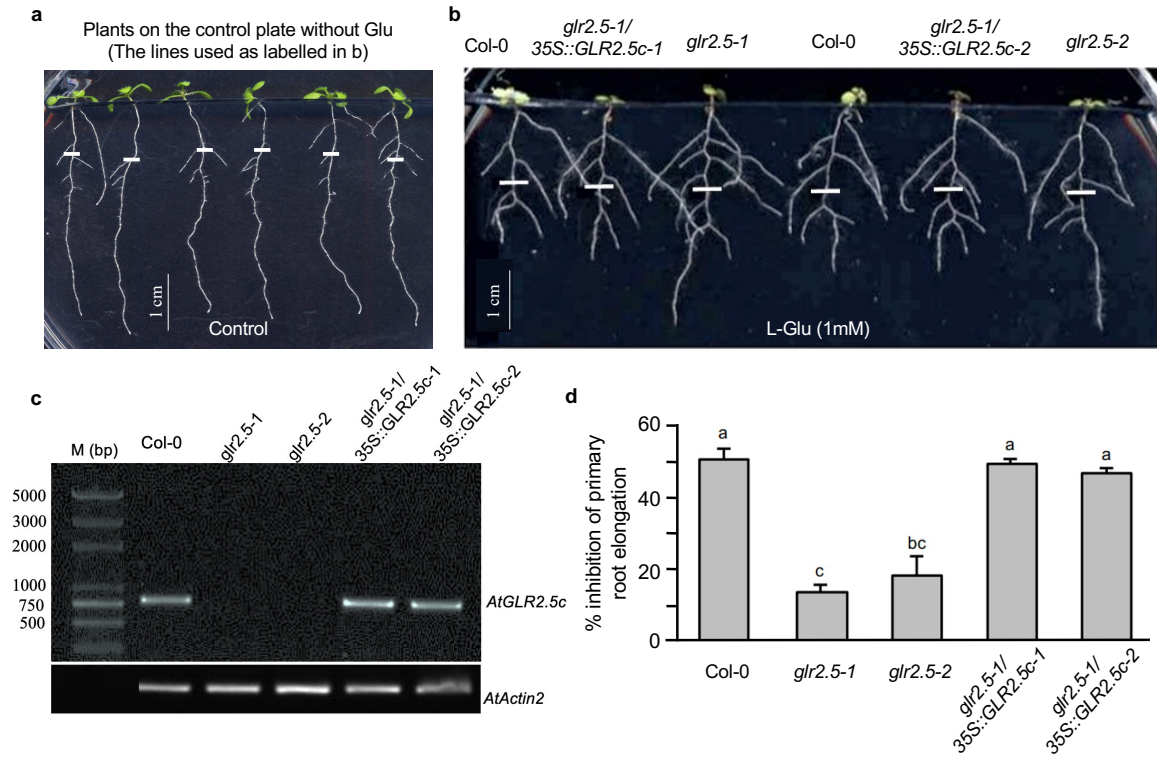

FIGURE 5 Complementation of a *glr2.5* mutant by transformation with the *35S*::*GLR2.5c* construct. A construct carrying the enhanced CaMV 35S promoter fused to the *GLR2.5c* cDNA sequence (*35S::GLR2.5c*) was used to transform the *glr2.5-1* mutant and two independent transgenic lines (*glr2.5*/*35S::GLR2.5c-1* and *glr2.5*/*35S::GLR2.5c-2*) were analysed. (**a**, **b**) Representative images of seedlings of Col-0, the *glr2.5-1* mutant and the complemented lines 4 d-old seedlings were grown on vertical agar plates and transferred to plates ± 1 mM L-Glu for a further 6 d. Horizontal lines show the positions of the primary root tips at the time of transfer. Plant growth test was conducted as did for Figure 2 (**c**) Detection of *GLR2.5c* expression in different lines. RT-PCR was performed on total RNA extracted from seedlings of the *glr2.5* mutants, the *GLR2.5c*-transformed complementation lines and their wide-type Col-0. Two primers (5'-ATGGCTTCAAGACAAGGATTG-3', 5'-CTAGTGGAAATGCAAAGCCA-3') designed specifically for the detection of *GLR2.5c*-derived fragment (808 bp predicted) were used. PCR products were separated by gel electrophoresis and stained with ethidium bromide. Upper panel: products obtained using PCR primers to amplify the *GLR2.5c*-derived sequence; and amplicons were isolated from gel and sequenced to verify their sequence correctness (808 bp indeed as the predicted). Lower panel: RNA quality control showing products obtained with *Actin2* primers (see Materials and Methods). (**d**) Quantification of the primary root elongation. Quantitative data from the same experiment as did for b. Primary root elongation over the following 6 d was measured, and

471 percentage inhibition by L-Glu was calculated for each line by comparison with the control (no
472 L-Glu) plates (± SE; n=18 plants). Different letters above bars show statistically significant
473 differences ($P < 0.05$, by one-way ANOVA).
474
475 **3.6 | Electrophysiological evidence of a role for the *GLR2.5* gene product in glutamate-**
476 **gated Ca^{2+} channel activity at the root tip**
477 Patch-clamping has been used to demonstrate glutamate-activated Ca^{2+} currents across the
478 plasma membrane of root protoplasts (Demidchik et al., 2004) and to provide direct *in planta*
479 evidence that proteins encoded by the *GLR3.1* and *GLR3.5* genes form L-Met-activated Ca^{2+}-
480 permeable channels in protoplasts from stomatal guard cells (Kong et al., 2016). Here we have
481 used this technique to investigate the effect of disruption of the *GLR2.5* gene on glutamate-
482 activated Ca^{2+} channel activity in root tip protoplasts and to assess the ability of the *GLR2.5g*
483 genomic clone and the constitutively expressed *GLR2.5c* cDNA to rescue the *glr2.5* mutant.
484 Protoplasts from Col-0, the *glr2.5-1* mutant and the complemented lines were subjected to
485 voltage-clamping to construct current-voltage relationships (*I-V* curves) from whole-cell
486 currents after L-Glu treatment (Figure 6). The results show that inactivation of the *GLR2.5*
487 gene in the *glr2.5-1* mutant was sufficient to eliminate glutamate-activated Ca^{2+} channel
488 activity in the root tip protoplasts (Figure 6a). Furthermore, this channel activity was fully
489 restored in *glr2.5-1* lines complemented with either the *GLR2.5g* genomic clone or the
490 constitutively expressed *GLR2.5c* cDNA. These results indicate that the *GLR2.5* gene product,
491 specifically the unusual product of the third largest of its four transcripts (*GLR2.5c*), either
492 operates as a glutamate-activated Ca^{2+}-permeable channel in the root tip (independently of the
493 products of the other three transcripts) or is required for such a channel to be functional.

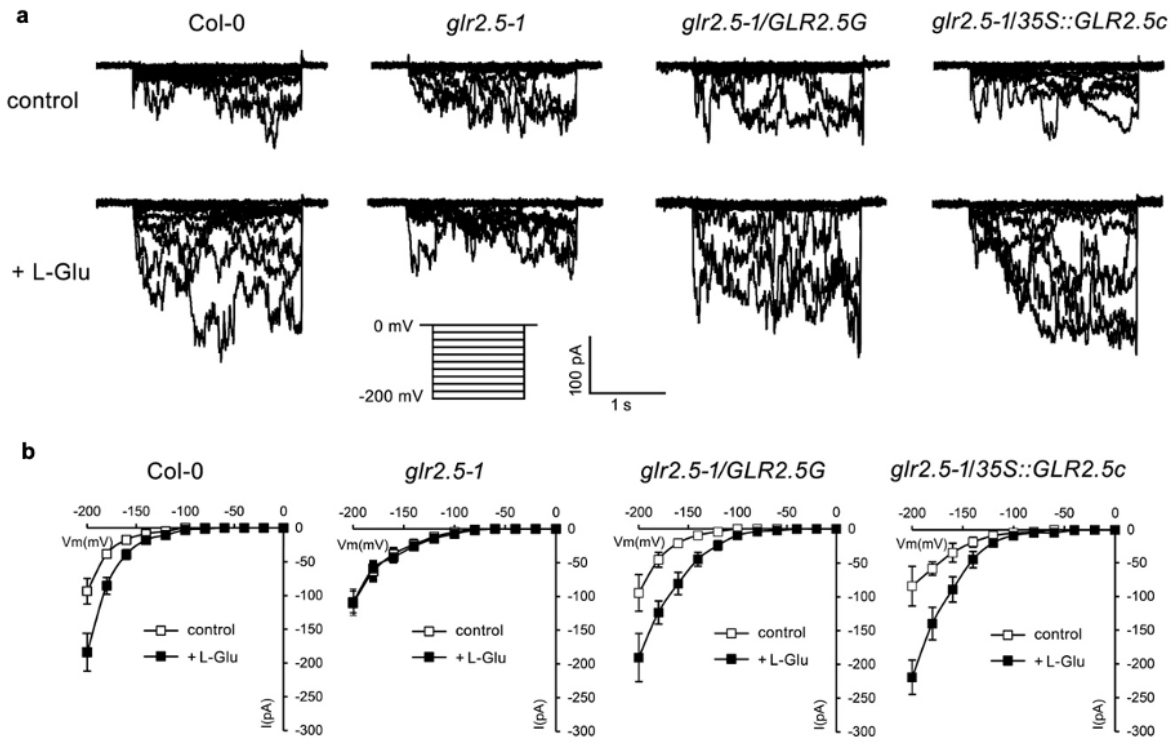

FIGURE 6 Glutamate-activation of inward Ca^{2+} currents in the plasma membrane of root protoplasts from Col-0, the *glr2.5-1* mutant and two complemented lines. Protoplasts from primary root tips of 15 d-old seedlings of Col-0, the *glr2.5-1* mutant and the *glr2.5-1*/*GLR2.5g* and *glr2.5-1*/*35S::GLR2.5c* lines were isolated and patch-clamped in whole-cell configuration as described in Methods. (**a**) Typical time course of changes in Ca^{2+}-related currents in protoplasts from each line after treatment with 1 mM L-Glu or untreated (control). (**b**) Standardized current-voltage curves from a voltage-step experiment using protoplasts in the presence or absence of 1 mM L-Glu (+/- SE; n = 6-8, the number of protoplasts that showed the response to external L-Glu; and ten to fifteen protoplasts from each tested line were analysed).

3.7 | Homology modelling of the ligand-binding domains of GLR2.5 and GLR2.5c

Considering the evidence that GLR2.5c has a role in L-Glu sensing at the root tip, we wished to assess the likely effect that its truncated LBD would have on its ability to be activated by L-Glu. Homology modelling of the LBDs of plant GLRs has been greatly facilitated by the recent determination of the crystal structures of the LBDs of GLR3.3 (Alfieri et al., 2020) and GLR3.2 (Gangwar et al., 2021) together with the high degree of sequence conservation within the GLR

family, which allows domain boundaries to be reliably defined by sequence alignment (Alfieri et al., 2020; Grenzi et al., 2021).

The crystal structure of the GLR3.3 LBD was determined using a fusion protein made up of its S1 and S2 segments joined by a Gly-Gly-Thr linker (Alfieri et al., 2020) and the equivalent (hypothetical) fusion proteins based on the S1 and S2 segments of GLR2.5 and GLR2.5c (see Figure S7) were therefore used here to model the 3D structures of their LBDs. Full details of the sequences used for homology modelling are given in Figure S7. The LBDs of GLR2.5 and GLR3.3 have only a 38% sequence identity, but Figure 7a shows how the predicted 3D structure of the GLR2.5 LBD closely aligns with the experimentally determined structure of the GLR3.3 LBD. Figure 7B shows the GLR2.5 LBD on its own, with the N-terminal portion of the S1 segment that is missing in GLR2.5c being indicated in yellow. Other than this missing part of S1, the GLR2.5 and GLR2.5c models are identical. The reliability scores for both GLR2.5 models in Figure 7b are high, with a GMQE (Global Model Quality Estimation) of *ca* 0.75 and a QMEAN (Qualitative Model Energy Analysis) Z-score of *ca* -2.0 (Waterhouse et al., 2018). Notably, the structure of our GLR2.5 model is highly similar (root mean square deviation of 2.0 Å in the LBD region) to the structure of GLR2.5 predicted by the recently released neural network-based AlphaFold program (Jumper et al., 2021). By careful inspection of the L-Glu binding site in the models, the specific GLR3.3 residues involved in L-Glu binding (Phe133, Arg88, Ala83, Asp81, Glu177, Tyr180, Gln129, Arg11, Asn60, Tyr63; Alfieri et al., 2020) have unambiguously corresponding residues in GLR2.5 (Phe138, Arg93, Thr88, Asp86, Glu181, Tyr184, Gln134, Lys11, Arg65, Tyr68, respectively), that are either identical or conservatively changed (Figure 7c). Three of these residues (Lys11, Arg65, Tyr68) are missing in GLR2.5c and are responsible for coordinating the L-Glu side chain; however, the six residues coordinating the invariant part of the ligand are retained in GLR2.5c. The model supports the absence of major steric hindrances in the binding site, suggesting that an intact GLR2.5 LBD would be likely to bind and be gated by L-Glu and that the truncated GLR2.5c LBD might retain the same property to some degree but has its binding site fully exposed to solvent (Figure 7d).

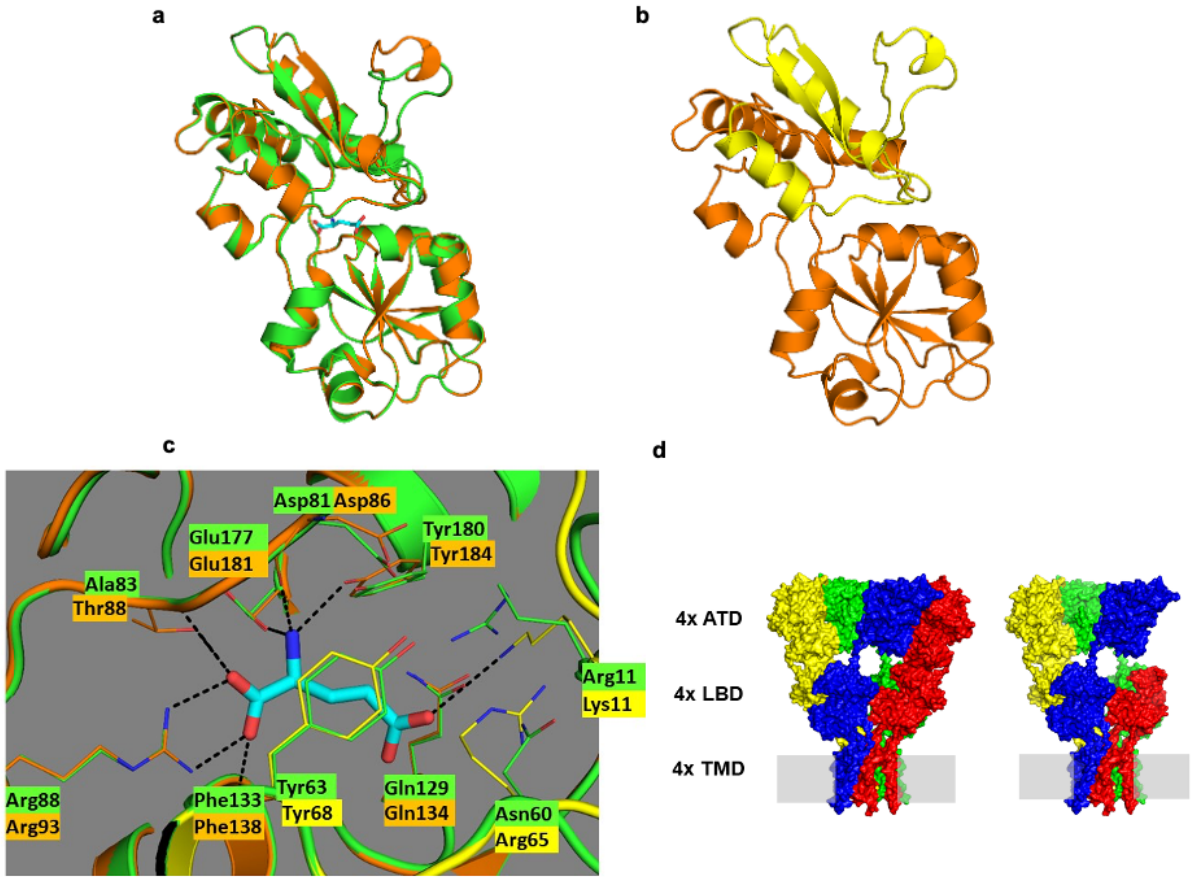

FIGURE 7 Homology modelling of the LBDs of the complete GLR2.5 protein and the truncated GLR2.5c protein. Homology modelling was based on the 3D structure of the GLR3.3 LBD and alignments with the predicted sequences of GLR2.5 (Aramemnon) and GLR2.5c (Figure S7). The models shown were prepared with PyMOL (The PyMOL Molecular Graphics System, Version 1.3 Schrödinger, LLC). (**a**) Superimposition of the experimentally determined structure of the LBD of GLR3.3 (green) and the model of the complete LBD of GLR2.5 (orange), in cartoon form. The L-Glu ligand bound to GLR3.3 is shown as light blue sticks. (**b**) Model of the GLR2.5 LBD with the yellow colour indicating the segment that is absent in GLR2.5c. (**c**) Close-up view of the binding site in the LBD of GLR3.3 (green) onto which the model of the complete LBD of GLR2.5 has been superimposed (orange/yellow). The main residues of GLR3.3 involved in binding the L-Glu ligand are indicated in green and the corresponding residues in GLR2.5 as orange or yellow. The residues of the GLR2.5 model indicated in yellow are those that are missing in GLR2.5c (Lys11, Arg65, Tyr68). Dotted black lines indicate bonds that are likely to coordinate an L-Glu ligand in GLR2.5. (**d**) (Left) Space-filling representation of a full GLR heterotetramer with each subunit in a different colour, based on the cryo-EM structure of the homotetrameric receptor GLR3.4 (Protein Data Bank ID 7LZH, (Green et al., 2021). Each subunit contributes one amino-terminal domain (ATD), one

ligand-binding domain (LBD) and one transmembrane domain (TMD). (Right) Space-filling representation, derived from the one above, of a hypothetical GLR heterotetramer where the red subunit is GLR2.5c, therefore lacking all the ATD and a portion of the LBD (the L-Glu ligand is white), but retaining the expected inter-subunit contact regions of the LBD and all the transmembrane helices.

4 | DISCUSSION

4.1 | GLR2.5 is involved in the root response to exogenous L-Glu

Previous physiological studies led to the conclusion that the Arabidopsis primary root tip is equipped with the ability to sense the external presence of L-Glu and to convert that signal into changes in root apical meristem activity, root tip morphology and lateral root outgrowth (Walch-Liu et al., 2006b). The specificity of the response implied the presence at the root tip of some form of L-Glu sensing mechanism, with the most promising candidate for the role of L-Glu sensor being the glutamate receptor-like proteins encoded by the family of 20 *GLR* genes, most of which are expressed in roots (Chiu et al., 2002). In the process of screening a collection of lines with T-DNA insertions in each of the 20 *GLR* genes we identified one gene, *GLR2.5*, whose disruption in two independent insertion mutants led to a significant decrease in the sensitivity of root growth to L-Glu (Figure 1). Disruption of *GLR2.5* almost eliminated the morphological changes at the root tip that are characteristic of Glu-treated roots (Figure 1d), yet the mutation had no effect on the root's sensitivity to a range of plant hormone treatments that inhibit root growth (Figure S3) or on its sensitivity to other amino acids (Figure 1c). That this reduction in sensitivity to L-Glu was due to the disruption of the *GLR2.5* gene itself was confirmed by the ability of a genomic fragment carrying the *GLR2.5* gene (*GLR2.5g*) to fully restore the wild-type phenotype when used to transform the *glr2.5* mutant (Figure 2). A previous study of natural variation in the sensitivity of Arabidopsis roots to L-Glu identified a number of QTLs, one of which mapped to the region of chromosome 5 containing the closely linked *GLR2.5* and *GLR2.6* genes (Walch-Liu et al., 2017), so that the present results are consistent with the possibility that natural variants of the *GLR2.5* gene are responsible for this QTL.

It should be noted that although we found no evidence that T-DNA insertions in any of the other 19 *GLR* genes affected the sensitivity of root growth to L-Glu, the remarkable sensitivity of this trait to genotype x environment interactions (Walch-Liu et al., 2017) means

that we cannot eliminate the possibility that effects of mutations in other *GLR* genes might be uncovered under different environmental conditions or in different genetic backgrounds.

GLR2.5, like most clade 2 genes, is preferentially expressed in roots (Chiu et al., 2002) and belongs to a set of genes positively regulated by G-Box Binding Factor 3 (*GBF3*), a transcription factor involved in the plant's responses to multiple biotic and abiotic stresses (Dixit et al., 2019). This is consistent with transcriptomics data (http://bar.utoronto.ca/eplant) showing that *GLR2.5* expression in roots is strongly induced by both cold and salt treatments as well as by a variety of pathogen-related signals such as the immunity elicitor flg22. In this context it is noteworthy that three genes established as downstream components in the root tip response to L-Glu (*MEKK1*, *MPK6* and *MKP1*) (Forde et al., 2013; Lopez-Bucio et al., 2018) encode components of MAP kinase signalling pathways involved in the innate immune response (Asai et al., 2002). Given other evidence that exogenous glutamate applied to roots can trigger defence responses in Arabidopsis (Goto et al., 2020) and other plant species (Kadotani et al., 2016; Kan et al., 2017; Sun et al., 2019), it would not be surprising if *GLR2.5* had a wider role in L-Glu signalling, beyond its role in the root architectural response. Recently the tandemly arranged *GLR2.7/2.8/2.9* genes have been shown to have a role in pattern-triggered immunity (Bjornson et al., 2021).

4.2 | Significance of the spatial localization of *GLR2.5* expression

We used a *GLR2.5pro::GUS* reporter gene to investigate the pattern of *GLR2.5* expression in Arabidopsis roots, finding that its expression was strongest in the outer layers of the primary root tip (Figure 3). This is consistent with earlier cell type-specific microarray data that showed *GLR2.5* expression to be strongest in cells of the stage 1 lateral root cap (LRC), the section of the LRC closest to the primary root apex, where it was also one of the most highly expressed of the 19 Arabidopsis *GLR* genes for which data was presented (Brady et al., 2007). This pattern of localization of *GLR2.5* expression is also in line with experimental data showing that external L-Glu is sensed specifically at the root apex (Walch-Liu et al., 2006b).

There is accumulating evidence that the LRC has a key role to play in regulating root meristematic activity through hormone-mediated pathways (Di Mambro et al., 2019; Pierdonati et al., 2019). In this study, since the introduction of a construct of *GLR2.5g* (containing a native promoter sequence) or *35S::GLR2.5c* into the *glr2.5-1* mutant line leads to a full recovery of the root system growth sensitivity of mutant plants to external L-Glu (Figure 2, Figure 5), and since *GLR2.5* promoter activity apparently occurs also in the lateral root apex (Figure 3c), one

may argue that the expression of *GLR2.5* in the LRC would place it in the prime location for regulating meristematic activity in response to changes in external L-Glu concentration at the root tip. However, this speculation is awaiting experimental elucidation in a future work.

4.3 | Four alternative splice variants of *GLR2.5* in Arabidopsis roots

Cloning and sequence analysis of four splice variants of the *GLR2.5* gene (*GLR2.5a-d*; Figure 4a) revealed that none correspond to the 2490 bp mRNA predicted from the gene model in the Aramemnon database [https://aramemnon.botanik.uni-koeln.de] and that they arise from a combination of exon skipping, intron retention and use of alternative splice donor sites (Figure 4B and Figure S4). In the case of the *GLR2.5c* and *GLR2.5d* transcripts, more than one type of event was responsible for the final transcript. Surprisingly, although two of the alternative splicing events (in *GLR2.5a* and *GLR2.5b*) produce frameshifts and termination of translation >400 nucleotides upstream of the predicted stop codon, these transcripts are apparently not targeted for nonsense-mediated decay (Kalyna et al., 2012).

There is increasing recognition of the importance of alternative splicing in plant development and in the plant's response to environmental signals (Shang et al., 2017; Martin et al., 2021). Alternative splicing of the *GLR3.5* gene transcript has been found to produce two variant proteins, one of which is targeted to the mitochondria and the other to the chloroplast (Teardo et al., 2015). Alternative splicing in mammalian iGluRs is frequently used to generate isoforms with different properties (Traynelis et al., 2010). For example, a truncated isoform of a mammalian AMPA receptor acts in a dominant negative fashion to produce non-functional heteromeric receptors (Gomes et al., 2008) and an isoform of a rat NMDA receptor with a modified version of the ATD alters its allosteric regulation (Traynelis et al., 1995). In the case of GLR2.5, only one of the four predicted proteins (GLR2.5c) possesses all the conserved regions that are characteristic of both plant GLRs and animal iGluRs (Figure 4). With all membrane-spanning regions present, as well as an intact P region, GLR2.5c is the isoform with the greatest potential to act as a functional Ca^{2+}-permeable channel, although the absence of almost the entire ATD and the first part of the S2 segment raises questions about its properties. Notably, in none of the four predicted proteins are the complete S1 and S2 segments of the LBD both intact.

4.4 | Evidence of a specific role for the *GLR2.5c* transcript in the root response to L-Glu

655 We were able to demonstrate that expressing the *GLR2.5c* transcript under the control of the
656 constitutive 35S promoter can fully restore L-Glu sensitivity of root growth in a *glr2.5* mutant
657 background (Figure 5). Because the primary root apex is the only part responsible for root
658 growth sensitivity to L-Glu (Walch-Liu et al., 2006), and *GLR2.5* promoter activity is
659 apparently detected in the root tip zone (Figure 3), a constitutive *GLR2.5c* expression triggered
660 by the 35S promoter might not ectopically affect GLR2.5c function within the root tip in
661 response to external L-Glu. Furthermore, when the *glr2.5-1* mutant was complemented with
662 either the *35S::GLR2.5c* construct or the *GLR2.5* genomic fragment (*GLR2.5g*), patch-
663 clamping at the single channel level in root tip protoplasts showed that L-Glu-elicited Ca^{2+}
664 currents that were lost in the mutant had been restored (Figure 6). The existence in Arabidopsis
665 roots of L-Glu-elicited Ca^{2+} currents that are accompanied by rapid changes in membrane
666 potential is well-established (Dennison & Spalding, 2000; Demidchik et al., 2004) and
667 knockout mutants in both *GLR3.3* (Qi et al., 2006) and *GLR3.6* (Singh et al., 2016) have been
668 found to be defective in these electrophysiological responses at the root tip. There is
669 experimental evidence that plant GLRs, like their mammalian iGluR counterparts (Glasgow et
670 al., 2015), operate as heterotetramers containing at least two types of subunit (Vincill et al.,
671 2012; Price & Okumoto, 2013; Vincill et al., 2013). Since both *GLR3.3* and *GLR3.6* appear to
672 be involved in conducting L-Glu-elicited Ca^{2+} currents at the root tip, the finding here that L-
673 Glu-elicited channel activity is lost in the *glr2.5-1* mutant suggests that GLR2.5c may be a
674 necessary component of heterotetrameric complexes with GLR3.3 and GLR3.6.
675 We were able to show by homology modelling that the predicted 3D structure of the
676 LBD of GLR2.5 is very similar to that of GLR3.3 (Figure 7a), which has an LBD that is not
677 only able to bind L-Glu but also a number of other amino acids (Alfieri *et al.*, 2020). However,
678 modelling of the truncated LBD of GLR2.5c (Figure 7b, c) suggests that its ability to bind L-
679 Glu is likely to be significantly weaker, owing to the absence of over half the S1 segment,
680 within which occur 3 of the 10 residues expected to coordinate binding of the L-Glu molecule.
681 Indeed, the absence of that portion of sequence in GLR2.5c might prevent the LBD operating
682 as a 'Venus flytrap' upon ligand binding, as seen in mammalian glutamate receptors (Acher &
683 Bertrand, 2005). Nevertheless, GLR2.5c is the only one of the four detected *GLR2.5* transcripts
684 that encodes the complete set of transmembrane helices and the P domain (Figure 4). In
685 addition, GLR2.5c apparently retains all the secondary structures mediating inter-subunit
686 contacts in the context of a tetramer (Figure 7d), based on the recently published structure of a
687 complete homotetramer of GLR3.4 obtained by cryo-electron microscopy (Green et al., 2021).
688 Thus, it is reasonable to expect that GLR2.5c could be assembled into heterotetramers (for

example with GLR3.3 and/or GLR3.6 subunits), but that any role for GLR2.5c in such a tetrameric complex is likely to be a regulatory or scaffolding one.

A previous study found that disruption of the *GLR3.3* gene led to a decrease in Glu-elicited membrane depolarization at the root tip and blocked the associated increase in cytosolic Ca^{2+} (Qi et al., 2006), so our finding that two independent *glr3.3* mutants were still sensitive to L-Glu (Figure S8) indicates that the Glu-elicited Ca^{2+} fluxes that are GLR3.3-dependent are not essential for L-Glu inhibition of root growth. That disruption of a single *GLR2.5* gene has such a significant effect on L-Glu sensitivity indicates that other *GLR* genes are unable to compensate for its absence, despite evidence that each of the other 19 *GLR* genes are expressed to varying levels in roots (Chiu et al., 2002). However, it is important to note that a distinction needs to be made between responses to short-term exposure to external L-Glu (such as seen when measuring Ca^{2+} fluxes, electrical responses or rapid changes in gene expression) and the effects of L-Glu on root development, which follow several days of exposure to the amino acid (Walch-Liu et al., 2006b). For example, it is a characteristic of ligand-gated channels that prolonged or repetitive stimulation by an agonist leads to desensitization of the receptor and a consequent reduction in the downstream response (Traynelis et al., 2010). Thus, long-term exposure to L-Glu may result in partial or complete desensitization of some of the GLR receptor isoforms present at the root apex. Additionally, over a period of hours and days, the sustained presence of external L-Glu is likely to result in metabolic, transcriptional or post-transcriptional changes that, in turn, lead to changes in the structure, subunit composition and/or relative abundance of different isoforms of the GLR receptors at the root tip.

Previous studies have shown that L-Glu is the only amino acid able to elicit the characteristic changes in root architecture (Walch-Liu et al., 2006b; Forde, 2014), yet it is known that the GLR family as a group is gated by a wide range of amino acids (Forde & Roberts, 2014). To explain this apparent paradox in the light of the new findings reported here, we suggest that the architectural response to L-Glu is either dependent on a very specific class of GLR2.5c-dependent heteromeric GLR channel that is only gated by L-Glu, or that gating of a GLR2.5c-dependent heteromeric channel by L-Glu produces a highly specific Ca^{2+} signature that is decoded to produce the appropriate phenotypic response (McAinsh & Pittman, 2009).

ACKNOWLEDGEMENTS

We thank the European Arabidopsis Stock Centre and the University of Bielefeld Arabidopsis Biological Resource Centre for providing the T-DNA insertional Arabidopsis lines. We are very grateful to Dr Pia Walch-Liu (Lancaster University, UK) for her contribution to the

isolation and screening of the T-DNA insertion mutants. We also thank Prof. Alex Costa (University of Milan) for valuable discussions. We gratefully acknowledge funding from the National Natural Science Foundation of China (grant no. 30771288 to L-H.L.), the Research Finding of Hunan Tobacco Science Institute (No. 19–22Aa02 and 2022433100240105), the Funding of China Tobacco Genome Project in China Tobacco Hunan Industrial Corporation (No. KY2022YC0006_110202201012(JY-12)), and the European Commission Research Training Network grant no. HPRN-CT-2002-00247 to B.G.F.

CONFLICT OF INTEREST STATEMENT

The authors declare no conflict of interest.

DATA AVAILABILITY STATEMENT

The data supporting the findings of this study are available in the supplementary materials of this article.

ORCID

Lai-Hua Liu**:** http://orcid.org/0000-0001-7650-0341

REFERENCES

Acher, F. & Bertrand, H. (2005) Amino acid recognition by Venus flytrap domains is encoded in an 8-residue motif. *Biopolymers*, 80, 357-366.

Alfieri, A., Doccula, F.G., Pederzoli, R., Grenzi, M., Bonza, M.C., Luoni, L. et al. (2020) The structural bases for agonist diversity in an Arabidopsis thaliana glutamate receptor-like channel. *Proceedings of the National Academy of Sciences of the United States of America,* 117, 752-760.

Alonso, J.M., Stepanova, A.N., Leisse, T.J., Kim, C.J., Chen, H.M., Shinn, P. et al.(2003) Genome-wide insertional mutagenesis of *Arabidopsis thaliana*. *Science,* 301, 653-657.

Aouini, A., Matsukura, C., Ezura, H., Asamizu, E. (2012) Characterisation of 13 glutamate receptor-like genes encoded in the tomato genome by structure, phylogeny and expression profiles. *Gene*, 493(1), 36-43.

Asai, T., Tena, G., Plotnikova, J., Willmann, M.R., Chiu, W.L., Gomez-Gomez, L. et al. (2002) MAP kinase signalling cascade in Arabidopsis innate immunity. *Nature*, 415, 977-983.

Benkert, P., Biasini, M. & Schwede, T. (2011) Toward the estimation of the absolute quality of individual protein structure models. *Bioinformatics*, 27, 343-350.

Bjornson, M., Pimprikar, P., Nuernberger, T. & Zipfel, C. (2021) The transcriptional landscape of *Arabidopsis thaliana* pattern-triggered immunity. *Nature Plants*, 7, 579-586.

Brady, S.M., Orlando, D.A., Lee, J.Y., Wang, J.Y., Koch, J., Dinneny, J.R. et al. (2007) A high-resolution root spatiotemporal map reveals dominant expression patterns. *Science*, 318, 801-806.

Chiu, J., DeSalle, R., Lam, H.M., Meisel, L. & Coruzzi, G. (1999) Molecular evolution of glutamate receptors: A primitive signaling mechanism that existed before plants and animals diverged. *Molecular Biology and Evolution*, 16, 826-838.

Chiu, J.C., Brenner, E.D., DeSalle, R., Nitabach, M.N., Holmes, T.C. & Coruzzi, G.M. (2002) Phylogenetic and expression analysis of the glutamate receptor-like gene family in *Arabidopsis thaliana*. *Molecular Biology and Evolution*, 19, 1066-1082.

Davenport, R. (2002) Glutamate receptors in plants. *Annals of Botany*, 90, 549-557.

Demidchik, V., Bowen, H.C., Maathuis, F.J.M., Shabala, S.N., Tester, M.A., White, P.J. et al. (2002) *Arabidopsis thaliana* root non-selective cation channels mediate calcium uptake and are involved in growth. *Plant Journal*, 32, 799-808.

Demidchik, V., Essah, P.A. & Tester, M. (2004) Glutamate activates cation currents in the plasma membrane of Arabidopsis root cells. *Planta*, 219, 167-175.

Dennison, K.L. & Spalding, E.P. (2000) Glutamate-gated calcium fluxes in Arabidopsis. *Plant Physiology*, 124, 1511-1514.

Di Mambro, R., Svolacchia, N., Dello Ioio, R., Pierdonati, E., Salvi, E., Pedrazzini, E. et al. (2019) The lateral root cap acts as an auxin sink that controls meristem size. *Current Biology*, 29, 1199-1205.

Dixit, S.K., Gupta, A., Fatima, U. & Senthil-Kumar, M. (2019) AtGBF3 confers tolerance to *Arabidopsis thaliana* against combined drought and *Pseudomonas syringae* stress. *Environmental and Experimental Botany*, 168, 103881.

Drew, M.C. (1975) Comparison of the effects of a localized supply of phosphate, nitrate, ammonium and potassium on the growth of the seminal root system, and the shoot, in barley. *New Phytologist*, 75, 479-490.

Drew, M.C., Saker, L.R. & Ashley, T.W. (1973) Nutrient supply and the growth of the seminal root system in barley. I. The effect of nitrate concentration on the growth of axes and laterals. *Journal of Experimental Botany*, 24, 1189-1202.

788 Duan, Y.H., Li, F.N., Tan, K.R., Liu, H.N., Li, Y.H., Liu, Y.Y. et al. (2015) Key mediators of
789 intracellular amino acids signaling to mTORC1 activation. *Amino Acids*, 47, 857-867.
790 Forde, B.G. (2014) Glutamate signalling in roots. *Journal of Experimental Botany*, 65, 779-
791 787.
792 Forde, B.G., Cutler, S., Zaman, N. & Krysan, P.J. (2013) Glutamate signalling via a MEKK1
793 kinase-dependent pathway induces changes in *Arabidopsis* root architecture. *Plant*
794 *Journal*, 75, 1-10.
795 Forde, B.G. & Roberts, M.R. (2014) Glutamate receptor-like channels in plants: a role as amino
796 acid sensors in plant defence? *F1000 Prime Reports*, 6, 37.
797 Gangwar, S.P., Green, M.N., Michard, E., Simon, A.A., Feijo, J.A. & Sobolevsky, A.I. (2021)
798 Structure of the Arabidopsis Glutamate Receptor-Like Channel GLR3.2 ligand-binding
799 domain. *Structure*, 29, 161-169.
800 Glasgow, N.G., Retchless, B.S. & Johnson, J.W. (2015) Molecular bases of NMDA receptor
801 subtype-dependent properties. *Journal of Physiology-London*, 593, 83-95.
802 Gomes, A.R., Ferreira, J.S., Paternain, A.V., Lerma, J., Duarte, C.B. & Carvalho, A.L. (2008)
803 Characterization of alternatively spliced isoforms of AMPA receptor subunits encoding
804 truncated receptors. *Molecular and Cellular Neuroscience*, 37, 323-334.
805 Goto, Y., Maki, N., Ichihashi, Y., Kitazawa, D., Igarashi, D., Kadota, Y. et al. (2020)
806 Exogenous treatment with glutamate induces immune responses in arabidopsis. *Molecular*
807 *Plant-Microbe Interactions*, 33, 474-487.
808 Green, M.N., Gangwar, S.P., Michard, E., Simon, A.A., Portes, M.T., Barbosa-Caro, J. et al.
809 (2021) Structure of the *Arabidopsis thaliana* Glutamate Receptor-Like channel GLR3.4.
810 *Molecular Cell*, 81, 3216-3226.
811 Grenzi, M., Bonza, M.C., Alfieri, A. & Costa, A. (2021) Structural insights into long-distance
812 signal transduction pathways mediated by plant glutamate receptor-like channels. *New*
813 *Phytologist*, 229, 1261-1267.
814 Haddad, J.J. (2005) N-methyl-D-aspartate (NMDA) and the regulation of mitogen-activated
815 protein kinase (MAPK) signaling pathways: A revolving neurochemical axis for
816 therapeutic intervention? *Progress in Neurobiology*, 77, 252-282.
817 Hellens, R.P., Edwards, E.A., Leyland, N.R., Bean, S. & Mullineaux, P.M. (2000) pGreen: a
818 versatile and flexible binary Ti vector for Agrobacterium-mediated plant transformation.
819 *Plant Molecular Biology*, 42, 819-832.
820 Ju, C.L., Song, Y.N. & Kong, D.D. (2020) Arabidopsis GLR3.5-modulated seed germination
821 involves GA and ROS signaling. *Plant Signaling & Behavior*, 15, 1729537.

822 Jumper, J., Evans, R., Pritzel, A., Green, T., Figurnov, M., Ronneberger, O. et al. (2021) Highly
823 accurate protein structure prediction with AlphaFold. *Nature*, 596, 583-589.
824 Kadotani, N., Akagi, A., Takatsuji, H., Miwa, T. & Igarashi, D. (2016) Exogenous
825 proteinogenic amino acids induce systemic resistance in rice. *Bmc Plant Biology*, 16, 60.
826 Kalyna, M., Simpson, C.G., Syed, N.H., Lewandowska, D., Marquez, Y., Kusenda, B. et al.
827 (2012) Alternative splicing and nonsense-mediated decay modulate expression of
828 important regulatory genes in Arabidopsis. *Nucleic Acids Research*, 40, 2454-2469.
829 Kan, C.C., Chung, T.Y., Wu, H.Y., Juo, Y.A. & Hsieh, M.H. (2017) Exogenous glutamate
830 rapidly induces the expression of genes involved in metabolism and defense responses in
831 rice roots. *Bmc Genomics*, 18, 186.
832 Kang, J.M., Mehta, S. & Turano, F.J. (2004) The putative glutamate receptor 1.1 (AtGLR1.1)
833 in *Arabidopsis thaliana* regulates abscisic acid biosynthesis and signaling to control
834 development and water loss. *Plant and Cell Physiology*, 45, 1380-1389.
835 Kay, R., Chan, A., Daly, M. & McPherson, J. (1987) Duplication of CaMV-35S promoter
836 sequences creates a strong enhancer for plant genes. *Science*, 236, 1299-1302.
837 Kleinboelting, N., Huep, G., Kloetgen, A., Viehoever, P. & Weisshaar, B. (2012) GABI-Kat
838 SimpleSearch: new features of the Arabidopsis thaliana T-DNA mutant database. *Nucleic*
839 *Acids Research*, 40, D1211-D1215.
840 Kong, D., Hu, H.C., Okuma, E., Lee, Y., Lee, H.S., Munemasa, S. et al. (2016) L-Met activates
841 Arabidopsis GLR Ca2+ channels upstream of ROS production and regulates stomatal
842 movement. *Cell Reports*, 17, 2553-2561.
843 Kong, D., Ju, C., Parihar, A., Kim, S., Cho, D. & Kwak, J.M. (2015) Arabidopsis glutamate
844 receptor homolog3.5 modulates cytosolic Ca^{2+} level to counteract effect of abscisic acid
845 in seed germination. *Plant Physiology*, 167, 1630-1642.
846 Li, J., Zhu, S., Song, X., Shen, Y., Chen, H., Yu J. et al. (2006) A rice glutamate receptor-like
847 gene is critical for the division and survival of individual cells in the root apical meristem.
848 *Plant Cell*, 18, 340-349.
849 Liu, S., Zhang, X., Xiao, S., Ma, J., Shi, W., Qin, T. et al. (2021) A Single-Nucleotide Mutation
850 in a GLUTAMATE RECEPTOR-LIKE Gene Confers Resistance to Fusarium Wilt in
851 *Gossypium hirsutum*. *Advanced Science (Weinh)*, 8(7):2002723.
852 Lopez-Bucio, J.S., Raya-Gonzalez, J., Ravelo-Ortega, G., Ruiz-Herrera, L.F., Ramos-Vega,
853 M., Leon, P. et al. (2018) Mitogen activated protein kinase 6 and MAP kinase phosphatase
854 1 are involved in the response of Arabidopsis roots to L-glutamate. *Plant Molecular*
855 *Biology*, 96, 339-351.

Mao, L.M., Tang, Q.S. & Wang, J.Q. (2009) Regulation of extracellular signal-regulated kinase phosphorylation in cultured rat striatal neurons. *Brain Research Bulletin* 78, 328-334.

Martin, G., Marquez, Y., Mantica, F., Duque, P. & Irimia, M. (2021) Alternative splicing landscapes in Arabidopsis thaliana across tissues and stress conditions highlight major functional differences with animals. *Genome Biology*, 22, 35.

McAinsh, M.R. & Pittman, J.K. (2009) Shaping the calcium signature. *New Phytologist*, 181, 275-294.

Medvedev, S.S. (2018) Principles of calcium signal generation and transduction in plant cells. *Russian Journal of Plant Physiology*, 65, 771-783.

Michard, E., Lima, P.T., Borges, F., Silva, A.C., Portes, M.T., Carvalho, J.E. et al. (2011) Glutamate receptor-like genes form Ca^{2+} channels in pollen tubes and are regulated by pistil D-serine. *Science*, 332, 434-437.

Nakanishi, N., Shneider, N. A., and Axel, R. (1990) A family of glutamate receptor genes: evidence for the formation of heteromultimeric receptors with distinct channel properties. Neuron 5, 569–581.

Pierdonati, E., Unterholzner, S.J., Salvi, E., Svolacchia, N., Bertolotti, G., Dello Ioio, R. et al. (2019) Cytokinin-dependent control of GH3 Group II family genes in the Arabidopsis root. *Plants-Basel*, 8, 94.

Price, M. & Okumoto, S. (2013) Inter-subunit interactions between Glutamate-Like Receptors in Arabidopsis. *Plant Signaling & Behavior*, 8, e27034.

Price, M.B., Jelesko, J. & Okumoto, S. (2012) Glutamate receptor homologs in plants: functions and evolutionary origins. *Frontiers in Plant Science*, 3, 235.

Qi, Z, Stephens, N.R. & Spalding, E.P. (2006) Calcium entry mediated by GLR3.3, an Arabidopsis glutamate receptor with a broad agonist profile. *Plant Physiology*, 142, 963-971.

Qiu, X.M., Sun, Y.Y., Ye, X.Y. & Li, Z.G. (2020) Signaling role of glutamate in plants. *Frontiers in Plant Science*, 10, 1743.

Ravelo-Ortega, G., Lopez-Bucio, J.S., Ruiz-Herrera, L.F., Pelagio-Flores, R., Ayala-Rodriguez, J.A., de la Cruz, H.R. et al. (2021) The growth of Arabidopsis primary root is repressed by several and diverse amino acids through auxin-dependent and independent mechanisms and MPK6 kinase activity. *Plant Science*, 302, 1110717.

Robinson, D. (1994) The responses of plants to non-uniform supplies of nutrients. *New Phytologist*, 127, 635-674.

889 Rosso, M.G., Li, Y., Strizhov, N., Reiss, B., Dekker, K. & Weisshaar, B. (2003) An
890 *Arabidopsis thaliana* T-DNA mutagenized population (GABI-Kat) for flanking sequence
891 tag-based reverse genetics. *Plant Molecular Biology*, 53, 247-259.
892 Roy, S.J., Gilliham, M., Berger, B., Essah, P.A., Cheffings, C., Miller, A.J. et al. (2008)
893 Investigating glutamate receptor-like gene co-expression in *Arabidopsis thaliana*. *Plant*
894 *Cell and Environment*, 31, 861-871.
895 Schwacke, R., Schneider, A., van der Graaff, E., Fischer, K., Catoni, E., Desimone, M. et al.
896 (2003) ARAMEMNON, a novel database for Arabidopsis integral membrane proteins.
897 *Plant Physiology*, 131, 16-26.
898 Shang, X.D., Cao, Y. & Ma, L.G. (2017) Alternative splicing in plant genes: a means of
899 regulating the environmental fitness of plants. *International Journal of Molecular*
900 *Sciences*, 18, 432.
901 Simon, A.A., Navarro-Retamal, C. & Feijó, J.A. (2023) Merging Signaling with Structure:
902 Functions and Mechanisms of Plant Glutamate Receptor Ion Channels. *Annual Review*
903 *of Plant Biology,* 74, 415-52.
904 Singh, S.K., Chien, C.T. & Chang, I.F. (2016) The Arabidopsis glutamate receptor-like gene
905 GLR3.6 controls root development by repressing the Kip-related protein gene KRP4.
906 *Journal of Experimental Botany*, 67, 1853-1869.
907 Skobeleva, O.V., Ktitorova, I.N. & Agal'tsov, K.G. (2011) The causes for barley root growth
908 retardation in the presence of ammonium and glutamate. *Russian Journal of Plant*
909 *Physiology*, 58, 307-315.
910 Stephens, N.R., Qi, Z. & Spalding, E.P. (2008) Glutamate receptor subtypes evidenced by
911 differences in desensitization and dependence on the *GLR3.3* and *GLR3.4* genes. *Plant*
912 *Physiology*, 146, 529-538.
913 Sun, C., Jin, L.F., Cai, Y.T., Huang, Y.N., Zheng, X.D. & Yu, T. (2019) L-Glutamate treatment
914 enhances disease resistance of tomato fruit by inducing the expression of glutamate
915 receptors and the accumulation of amino acids. *Food Chemistry*, 293, 263-270.
916 Tapken, D., Anschutz, U., Liu, L.H., Huelsken, T., Seebohm, G., Becker, D. et al. (2013) A
917 plant homolog of animal glutamate receptors is an ion channel gated by multiple
918 hydrophobic amino acids. *Science Signaling*, 6, ra47.
919 Teardo, E., Carraretto, L., De Bortoli, S., Costa, A., Behera, S., Wagner, R. et al. (2015)
920 Alternative splicing-mediated targeting of the Arabidopsis GLUTAMATE
921 RECEPTOR3.5 to mitochondria affects organelle morphology. *Plant Physiology*, 167,
922 216-227.

923 Teardo, E., Formentin, E., Segalla, A., Giacometti, G.M., Marin, O., Zanetti, M. et al. (2011)
924 Dual localization of plant glutamate receptor AtGLR3.4 to plastids and plasmamembrane.
925 *Biochimica et Biophysica Acta: Bioenergetics*, 1807, 359-367.
926 Traynelis, S.F., Hartley, M. & Heinemann, S.F. (1995) Control of proton sensitivity of the
927 NMDA receptor by RNA splicing and polyamines. *Science*, 268, 873-876.
928 Traynelis, S.F., Wollmuth, L.P., McBain, C.J., Menniti, F.S., Vance, K.M., Ogden, K.K. et al.
929 (2010) Glutamate receptor ion channels: structure, regulation, and function.
930 *Pharmacological Reviews*, 62, 405-496.
931 Turano, F.J., Panta, G.R., Allard, M.W. & van Berkum, P. (2001) The putative glutamate
932 receptors from plants are related to two superfamilies of animal neurotransmitter receptors
933 via distinct evolutionary mechanisms. *Molecular Biology and Evolution*, 18, 1417-1420.
934 Vincill, E.D, Bieck, A.M. & Spalding, E.P. (2012) Ca^{2+} conduction by an amino acid-gated ion
935 channel related to glutamate receptors. *Plant Physiology*, 159, 40-46.
936 Vincill, E.D., Clarin, A.E., Molenda, J.N. & Spalding, E.P. (2013) Interacting glutamate
937 receptor-like proteins in phloem regulate lateral root initiation in *Arabidopsis*. *Plant Cell*,
938 25, 1304-1313.
939 Walch-Liu, P. & Forde, B.G. (2007) L-Glutamate as a novel modifier of root growth and
940 branching: What's the sensor? *Plant Signaling and Behavior*, 2, 284-286.
941 Walch-Liu, P., Ivanov, I., Filleur, S., Gan, Y., Remans, T. & Forde, B.G. (2006a. Nitrogen
942 regulation of root branching. *Annals of Botany*, 97, 875-881.
943 Walch-Liu, P., Liu, L-H., Remans, T., Tester, M. & Forde, B.G. (2006b) Evidence that L-
944 glutamate can act as an exogenous signal to modulate root growth and branching in
945 *Arabidopsis thaliana*. *Plant and Cell Physiology*, 47, 1045-1057.
946 Walch-Liu, P., Meyer, R.C., Altmann, T. & Forde, B.G. (2017) QTL analysis of the
947 developmental response to L-glutamate in Arabidopsis roots and its genotype-by-
948 environment interactions. *Journal of Experimental Botany*, 68, 2919-2931.
949 Wang, J.Q., Fibuch, E.E. & Mao, L.M. (2007) Regulation of mitogen-activated protein kinases
950 by glutamate receptors. *Journal of Neurochemistry*, 100, 1-11.
951 Wang, W.H., Kohler, B., Cao, F.Q., Liu, G.W., Gong, Y.Y., Sheng, S. et al. (2012) Rice DUR3
952 mediates high-affinity urea transport and plays an effective role in improvement of urea
953 acquisition and utilization when expressed in Arabidopsis. *New Phytologist*, 193 (2012)
954 432–444.

955 Waterhouse, A., Bertoni, M., Bienert, S., Studer, G., Tauriello, G., Gumienny, R. et al. (2018)
956 SWISS-MODEL: homology modelling of protein structures and complexes. *Nucleic*
957 *Acids Research*, 46, W296-W303.
958 Wu, Q., Stolz, S., Kumari, A. & Farmer, E.E. (2022) The carboxy-terminal tail of GLR3.3 is
959 essential for wound response electrical signaling. *New Phytologist*, 236, 2189–201.
960 Weiland, M., Mancuso, S. & Baluska, F. (2016) Signalling via glutamate and GLRs in
961 *Arabidopsis thaliana*. *Functional Plant Biology*, 43, 1-25.
962 Wudick, M.M., Michard, E., Nunes, C.O. & Feijo, J.A. (2018) Comparing plant and animal
963 glutamate receptors: common traits but different fates? *Journal of Experimental Botany*,
964 69, 4151-4163.
965 Zhang, L., Qin, L., Zeng, Z., Wu, C., Gong, Y., Liu, L., et al. (2019) Molecular identification
966 of a root apical cell-specific and stress-responsive enhancer from an Arabidopsis enhancer
967 trap line. *Plant Methods* 15, 8. doi: 10.1186/s13007-019-0393-0.
968
969
970 **FIGURE 1** Disruption of the *GLR2.5* gene in two independent Arabidopsis T-DNA lines leads
971 to reduced glutamate sensitivity in primary root development. (**a**) Schematic representation of
972 two independent T-DNA insertion events in *GLR2.5* (At5g11210). The arrangement of exons
973 (E1-E6) is based on the model in the Aramemnon database [https://aramemnon.botanik.uni-
974 koeln.de]. The T-DNA insertions in the *glr2.5-1* and *glr2.5-2* lines (NASC accession nos
975 N578407 and N618122) are located respectively 2431 bp and 2585 bp downstream of the
976 predicted start of translation. Numbered arrows (P_1, P_2 for *glr2.5-1* and P_3, P_4 for *glr2.5-2*)
977 indicate annealing sites and orientations of PCR primers used to detect T-DNA insertions and
978 in homozygosity tests (for primer sequences see Table S1); P_T indicates the T-DNA primer
979 annealing site. The numbers indicate the nucleotide positions in the genomic sequence of
980 *AtGLR2.5* predicted in the Aramemnon. The expected DNA fragment size is 790 bp or 1049
981 bp between primer P_1 and P_2, or P_3 and P_4. L and R, left and right T-DNA borders. (**b**)
982 Representative image showing seedlings of Col-0 and the *glr2.5-1* and *glr2.5-2* mutants that
983 were germinated and grown for 4 d on vertical agar plates containing "standard medium"
984 (Walch-Liu et al., 2006b) and then transferred to plates ±1 mM L-Glu for a further 6 d (see
985 Materials and Methods). Horizontal dotted lines show the positions of the primary root tips at
986 the time of transfer. (**c**) Effect of other amino acids on root growth in the wild-type and the
987 two *glr2.5* mutants. The experiment was conducted as for the L-Glu treatment in b, except that
988 the respective amino acids were applied at a concentration of 0.5 mM. Data are means ± SE (n

=18 plants); different letters above bars indicate statistically significant differences ($P < 0.05$, by one-way ANOVA). (**d**) Close-ups of representative primary root tips of each line grown in the absent (Control) or presence of 1 mM L-Glu. Root materials were derived from the experiment for b.

FIGURE 2 Complementation of a *glr2.5* mutant by transformation with the *GLR2.5* gene. A construct carrying the *GLR2.5* gene as a 5533 bp genomic fragment (*GLR2.5g*) was used to transform the *glr2.5-1* mutant and two independent transgenic lines (*glr2.5*/*GLR2.5g-1* and *glr2.5*/*GLR2.5g-2*) were analyzed. (**a**) Detection of *GLR2.5* gene transcription. RT-PCR was performed on total RNA extracted from seedlings of the *glr2.5-1* and *glr2.5-2* mutants and from the two complemented lines as well as wide-type Col-0 (see Materials and Mehtods). PCR products were separated by gel electrophoresis and stained with ethidium bromide. Upper panel: products obtained using PCR primers designed to amplify the complete *GLR2.5* coding sequence; lower panel: RNA quality control showing products obtained with *Actin 2* primers. M, DNA marker. (**b**) Representative images of seedlings of Col-0, the *glr2.5-1* mutant and the complemented lines when 4 d-old seedlings were grown on vertical agar plates and transferred to plates ± 1 mM L-Glu for a further 6 d (see Materials and Methods). Horizontal lines show the positions of the primary root tips at the time of transfer. (**c**) Quantification of primary root growth. Plant data derived from the same experiments as for b. Primary root elongation over the following 5 d was measured, and percentage inhibition by L-Glu was calculated for each genotype by comparison with the control (no L-Glu) plates (± SE; n= 18 plants). Different letters above bars indicate statistically significant differences ($P < 0.05$, by one-way ANOVA). (d) Data showing the effect of L-Glu on meristematic activity in each line as measured by the mean distance from the root apex to the first root hair (± SE; n= 6-8 seedlings). Different letters above bars indicate statistically significant differences ($P < 0.05$, by one-way ANOVA).

FIGURE 3 Histochemical analysis of transgenic seedlings carrying the *GLR2.5pro::GUS* construct. Seedlings were germinated and grown on vertical agar plates containing standard nutrient medium and stained in 2 mM 5-bromo-4-chloro-3-indolyl β-d-glucuronide salt (X-Gal) at 37^{o} for 2 h incubation (Zhang et al., 2019). (**a**) Seedling 2 d after germination. (**b**) Seedling 3 d after germination. (**c**) Primary root of 8 d-old seedling. (**d**) Lateral root of 8 d-old seedling. (**e-g**) Transverse sections of the primary root apex of 8 d-old seedlings in the meristematic region (**e**) elongation zone (**f**) and root hair zone (**g**).

FIGURE 4 Cloning and characterization of four alternative *GLR2.5* transcripts. (**a**) RT-PCR was performed on total RNA from Arabidopsis seedlings to amplify the coding region of the *GLR2.5* gene and the products electrophoresed on agarose gels alongside a set of DNA markers (M) and stained with ethidium bromide. The four PCR products (*GLR2.5a*, *GLR2.5b*, *GLR2.5c* and *GLR2.5d*) were cloned and sequenced (Genbank accession nos JF838182, JF838183, JF838184 and JF838185, respectively). (**b**) Diagrammatic representation of the predicted arrangement of exons in *GLR2.5* based on the Aramemnon gene model (grey) [https://aramemnon.botanik.uni-koeln.de] and as seen in the four alternative transcripts (red). Numbering is from the start of the ATG codon in the *GLR2.5* genomic sequence and positions of the TAG stop codons in each transcript are indicated. Where exon skipping has occurred the intron is shown as an angled line. (**c**) Schematic diagram indicating the presence and absence of the conserved domains common to plant GLRs and animal iGluRs (see text and Figure S5) in the hypothetical translation products of each of the four alternative transcripts. Sequences present in each protein sequence are indicated in red, and sequences absent compared to the model are in grey. Where a frameshift occurs, this is indicated by a jagged line and the following 'nonsense' sequence by a wavy red line (see GlnH2 (S2) domain of 2.5a and 2.5b). Note: Numbering is from the N-terminus of the model GLR2.5 protein sequence (Aramemnon) and the conserved domains and their spacing are not drawn to scale. The ligand-binding subdomain GlnH1 (S1) and GlnH2 (S2) are early considered to have evolved from periplasmic binding proteins of bacteria due to their significant primary sequence similarity (Nakanishi et al., 1990).

FIGURE 5 Complementation of a *glr2.5* mutant by transformation with the *35S*::*GLR2.5c* construct. A construct carrying the enhanced CaMV 35S promoter fused to the *GLR2.5c* cDNA sequence (*35S::GLR2.5c*) was used to transform the *glr2.5-1* mutant and two independent transgenic lines (*glr2.5*/*35S::GLR2.5c-1* and *glr2.5*/*35S::GLR2.5c-2*) were analysed. (**a**, **b**) Representative images of seedlings of Col-0, the *glr2.5-1* mutant and the complemented lines 4 d-old seedlings were grown on vertical agar plates and transferred to plates ± 1 mM L-Glu for a further 6 d. Horizontal lines show the positions of the primary root tips at the time of transfer. Plant growth test was conducted as did for Figure 2 (**c**) Detection of *GLR2.5c* expression in different lines. RT-PCR was performed on total RNA extracted from seedlings of the *glr2.5* mutants, the *GLR2.5c*-transformed complementation lines and their wide-type Col-0. Two primers (5'-ATGGCTTCAAGACAAGGATTG-3', 5'-CTAGTGGAAATGCAAAGCCA-3') designed specifically for the detection of *GLR2.5c*-

derived fragment (808 bp predicted) were used. PCR products were separated by gel electrophoresis and stained with ethidium bromide. Upper panel: products obtained using PCR primers to amplify the *GLR2.5c*-derived sequence; and amplicons were isolated from gel and sequenced to verify their sequence correctness (808 bp indeed as the predicted). Lower panel: RNA quality control showing products obtained with *Actin2* primers (see Materials and Methods). (**d**) Quantification of the primary root elongation. Quantitative data from the same experiment as did for b. Primary root elongation over the following 6 d was measured, and percentage inhibition by L-Glu was calculated for each line by comparison with the control (no L-Glu) plates (± SE; n=18 plants). Different letters above bars show statistically significant differences ($P < 0.05$, by one-way ANOVA).

FIGURE 6 Glutamate-activation of inward Ca^{2+} currents in the plasma membrane of root protoplasts from Col-0, the *glr2.5-1* mutant and two complemented lines. Protoplasts from primary root tips of 15 d-old seedlings of Col-0, the *glr2.5-1* mutant and the *glr2.5-1*/*GLR2.5g* and *glr2.5-1*/*35S::GLR2.5c* lines were isolated and patch-clamped in whole-cell configuration as described in Methods. (**a**) Typical time course of changes in Ca^{2+}-related currents in protoplasts from each line after treatment with 1 mM L-Glu or untreated (control). (**b**) Standardized current-voltage curves from a voltage-step experiment using protoplasts in the presence or absence of 1 mM L-Glu (+/- SE; n = 6-8, the number of protoplasts that showed the response to external L-Glu).

FIGURE 7 Homology modelling of the LBDs of the complete GLR2.5 protein and the truncated GLR2.5c protein. Homology modelling was based on the 3D structure of the GLR3.3 LBD and alignments with the predicted sequences of GLR2.5 (Aramemnon) and GLR2.5c (Figure S7). The models shown were prepared with PyMOL (The PyMOL Molecular Graphics System, Version 1.3 Schrödinger, LLC). (**a**) Superimposition of the experimentally determined structure of the LBD of GLR3.3 (green) and the model of the complete LBD of GLR2.5 (orange), in cartoon form. The L-Glu ligand bound to GLR3.3 is shown as light blue sticks. (**b**) Model of the GLR2.5 LBD with the yellow color indicating the segment that is absent in GLR2.5c. (**c**) Close-up view of the binding site in the LBD of GLR3.3 (green) onto which the model of the complete LBD of GLR2.5 has been superimposed (orange/yellow). The main residues of GLR3.3 involved in binding the L-Glu ligand are indicated in green and the corresponding residues in GLR2.5 as orange or yellow. The residues of the GLR2.5 model

indicated in yellow are those that are missing in GLR2.5c (Lys11, Arg65, Tyr68). Dotted black lines indicate bonds that are likely to coordinate an L-Glu ligand in GLR2.5. (**d**) (Left) Space-filling representation of a full GLR heterotetramer with each subunit in a different colour, based on the cryo-EM structure of the homotetrameric receptor GLR3.4 (Protein Data Bank ID 7LZH, (Green et al., 2021). Each subunit contributes one amino-terminal domain (ATD), one ligand-binding domain (LBD) and one transmembrane domain (TMD). (Right) Space-filling representation, derived from the one above, of a hypothetical GLR heterotetramer where the red subunit is GLR2.5c, therefore lacking all the ATD and a portion of the LBD (the L-Glu ligand is white), but retaining the expected inter-subunit contact regions of the LBD and all the transmembrane helices.

SUPPORTING INFORMATION

FIGURE S1 Disruption of the *GLR2.5* gene in two independent T-DNA insertion mutants leads to a reduction in sensitivity of primary root elongation to L-Glu.

FIGURE S2 Effect of a *glr2.5* knock-out mutation on L-Glu sensitivity is independent of the background N source.

FIGURE S3 Effect of a range of hormone concentrations on primary root growth of Col-0 and the *glr2.5-1* mutant.

FIGURE S4 Multiple sequence alignment of the four alternative GLR2.5 cDNAs with the Aramemnon model cDNA sequence (At5g11210.1) and the *GLR2.5* genomic sequence (At5g11210).

FIGURE S5 Multiple sequence alignment of the four predicted GLR2.5 isoforms with the model GLR2.5 protein sequence.

FIGURE S6 No complementation of a *glr2.5* mutant by transformation with a construct harboring *35S::GLR2.5a, b or d*.

FIGURE S7 Sequences used in homology modelling.

FIGURE S8 The primary root growth of wild-type Col-0 and *glr3.3* mutant lines was sensitive to external L-Glu.

TABLE S1 Details of T-DNA insertion mutants in Arabidopsis *GLR* genes and the primers used to verify them.